

Library of FT-Raman spectra of pigments, minerals, pigment media and varnishes, and supplement to existing library of Raman spectra of pigments with visible excitation

Lucia Burgio¹, Robin J.H. Clark^{*}

Department of Chemistry, Christopher Ingold Laboratories, University College London, 20 Gordon Street, London WC1H 0AJ, UK

Received 29 August 2000; accepted 14 December 2000

Abstract

Sixty pigments, minerals and media have been analysed by Fourier-transform Raman (FT-Raman) microscopy in order to assemble a database of reference FT-Raman spectra for scientists working at the Arts–Science interface. An earlier library of Raman spectra compiled using visible excitation has been extended by the addition of 22 further reference spectra obtained with 780.0, 647.1, 632.8 and/or 514.5 nm excitation. The relative merits of 1064 nm and visible excitation are discussed. © 2001 Elsevier Science B.V. All rights reserved.

Keywords: Fourier-transform Raman (FT-Raman) microscopy; Raman spectra; Spectroscopic library; Pigments; Visible excitation

1. Introduction

The analysis of pigments on artworks is of major significance in art conservation as it leads to detailed characterisation of materials and is thus important for dating and authentication, as well as for possible conservation or restoration of artwork. Thus, a knowledge of the exact chemical nature of materials on works of art and of their

degradation products is critical in order to decide the conservation method to be employed. Several analytical techniques for the identification of pigments have been in use for many years; examples include polarised light microscopy (PLM), scanning electron microscopy (SEM) and energy-dispersive X-ray analysis (EDX), X-ray diffraction (XRD), X-ray fluorescence (XRF), Fourier-transform infrared spectroscopy (FT-IR), UV–visible absorption and fluorescence spectroscopy, and gas or liquid chromatography coupled to mass spectrometry. More recently, other techniques have been applied, viz. laser-induced breakdown spectroscopy (LIBS) [1,2], laser-induced fluorescence (LIF) [3], particle-induced X-ray emission (PIXE), particle-induced gamma-ray emission (PIGE), nu-

^{*} Corresponding author. Tel.: +44-20-76797457; fax: +44-20-76794603.

E-mail address: r.j.h.clark@ucl.ac.uk (R.J.H. Clark).

¹ Present address: Department of Conservation, Science Section, Victoria and Albert Museum, South Kensington, London SW7 2RL, UK.

Table 1
Blue pigments analysed with the Bruker FT-Raman spectrometer ($\lambda_0 = 1064 \text{ nm}$)

Name and composition	Band wavenumber ^a /cm ⁻¹ and relative intensity ^b	Experimental details ^c	Notes	Figure
<i>Azurite</i> basic copper(II) carbonate, $2\text{CuCO}_3 \cdot \text{Cu}(\text{OH})_2$	86m, 115vw, 137vw, 155vw, 177w, 249m, 282w, 332vw, 401vs, 739vw, 765w, 838w, 938w, 1096m, 1427m, 1459vw, 1578w	8 cm ⁻¹ , 16 mW, 500 scans	Mineral	Fig. 1
<i>Egyptian blue</i> calcium copper(II) silicate $\text{CaCuSi}_4\text{O}_{10}$	431m, 465m, 1086w	8 cm ⁻¹ , 3 mW, 500 scans	3000 BC. Mineral also known as cuprorivaite	Fig. 2
<i>Indigo</i> indigotin, $\text{C}_{16}\text{H}_{10}\text{N}_2\text{O}_2$	98w, 136w, 172vw, 181vw, 236w, 253m, 265w, 277w, 311w, 320vw, 468vw, 546m, 599m, 676w, 758w, 862vw, 871vw, 1015w, 1149vw, 1191vw, 1226w, 1248w, 1310m, 1363w, 1461w, 1483w, 1572vs, 1584s, 1626w, 1701w	2 cm ⁻¹ , 60 mW, 250 scans	Extract from plant leaf (BC)	Fig. 3
<i>Lazurite</i> S_3^- and S_2^- in a sodium alumino-silicate matrix, $\text{Na}_8[\text{Al}_6\text{Si}_6\text{O}_{24}]\text{S}_n$	352s(sh), 378s, 549s	8 cm ⁻¹ , 30 mW, 200 scans	Mineral lapis lazuli. Synthetic form 1828 (ultramarine blue)	Fig. 4

^a $\pm 1 \text{ cm}^{-1}$.

^b s, strong; m, medium; w, weak; v, very; sh, shoulder; br, broad.

^c Resolution, power at the sample, number of scans.

Table 2
Red pigments analysed with the Bruker FT-Raman spectrometer ($\lambda_0 = 1064 \text{ nm}$)

Name and composition	Band wavenumber ^a /cm ⁻¹ and relative intensity ^b	Experimental details ^c	Notes	Figure
<i>Carmin</i> carminic acid, C ₂₂ H ₂₀ O ₁₃	465w, 474w, 1108w, 1257m, 1314s, 1440m, 1489m, 1529m, 1645m	4 cm ⁻¹ , 16 mW, 2000 scans	Scale insect, cochineal (Aztec)	Fig. 5
<i>Kermes</i> kermesic acid, C ₁₆ H ₁₀ O ₈	1451vw, 1603w	4 cm ⁻¹ , 16 mW, 2000 scans	Scale insect, kermes (antiquity)	Fig. 6
<i>Litharge</i> tetragonal lead(II) oxide, PbO	83w, 147vs, 289vw, 339w	4 cm ⁻¹ , 270 mW, 100 scans	Antiquity	Fig. 7
<i>Madder</i> mainly alizarin, 1,2-dihydroxyanthraquinone, C ₁₄ H ₈ O ₄	239w, 485m, 841w, 1189m, 1221w, 1292m, 1327m, 1354w, 1482s, 1519m, 1577w, 1635w(br)	8 cm ⁻¹ , 26 mW, 100 scans	Dyestuff from the plant <i>Rubia Tinctorium</i>	Fig. 8
<i>Mars red</i> synthetic iron(III) oxide, Fe ₂ O ₃	294vw	8 cm ⁻¹ , 4 mW, 200 scans	Middle 19th C	Fig. 9
<i>Realgar</i> α -arsenic(II) sulfide, As ₄ S ₄	56vw, 61vw, 66vw, 125vw, 144m, 167w, 172w, 183s, 193s, 213vw, 231s, 329vw, 344m, 355s, 369w, 375vw	0.5 cm ⁻¹ , 8 mW, 100 scans	Mineral	Fig. 10
<i>Red lead</i> dilead(II) lead(IV) oxide, Pb ₃ O ₄	65w, 122vs, 144m, 148m, 150m, 224w, 232w(sh), 314w, 391w, 456vw, 477vw, 550vs	1 cm ⁻¹ , 14 mW, 100 scans	Antiquity	Fig. 11
<i>Tyrian purple</i> 6,6'-dibromo-indigotin, C ₁₆ H ₁₀ Br ₂ N ₂ O ₂	110m, 126m, 190m, 308m, 386w, 693m, 750m(sh), 760m, 1051m, 1105w, 1212w, 1254m, 1304w(sh), 1312w, 1366w, 1444w, 1565s(sh), 1584s, 1626w, 1702m	4 cm ⁻¹ , 8 mW, 2000 scans	Marine mollusc extract (1400 BC)	Fig. 12
<i>Vermilion</i> α -mercury(II) sulfide, HgS	253vs, 284w, 343m	1 cm ⁻¹ , 8 mW, 100 scans	Mineral (cinnabar) and synthetic (8th C)	Fig. 13

^a $\pm 1 \text{ cm}^{-1}$.

^b s, strong; m, medium; w, weak; v, very; sh, shoulder; br, broad.

^c Resolution, power at the sample, number of scans.

clear reaction analysis (NRA) and Rutherford back-scattering (RBS) [4–6]. Although valuable analytical results have been obtained with the above techniques, it is quite often necessary to employ more than one in order to achieve unambiguous results.

It should be noted that some of the techniques mentioned above are destructive, and/or necessitate sampling, which affects the integrity of the art object under analysis.

It has been proposed elsewhere that Raman microscopy is the ideal technique for the investigation of materials used on works of art [7–19] because it is very reliable, sensitive, specific, non-destructive and can be applied in situ, therefore avoiding any sampling and consequently any damage to the object under examination.

Fourier-transform Raman (FT-Raman) microscopy has only recently been employed for this

purpose [20,21]. Its main advantage over Raman microscopy employing visible excitation is that, by making use of infrared excitation, the problem of the fluorescence of materials under analysis can frequently be overcome. Moreover, the spectrometer system does not require frequent wavenumber calibration.

The authors have recently used FT-Raman microscopy in order to analyse manuscripts and other art objects [22]. This has revealed that the technique can be applied satisfactorily to the analysis of pigments and other materials, although it is not as fast as conventional Raman microscopy. No comprehensive libraries of FT-Raman spectra of artists' materials have as yet been published. This paper is supplemented by conventional Raman spectra of reference materials critically important to the analysis of art objects and additional to those published in our earlier library collection [23].

Table 3

White pigments analysed with the Bruker FT-Raman spectrometer ($\lambda_0 = 1064 \text{ nm}$)

Name and composition	Band wavenumber ^a /cm ⁻¹ and relative intensity ^b	Experimental details ^c	Notes ^d	Figure
<i>Anatase</i> titanium dioxide, TiO ₂	143vs, 396w, 516w, 639m	4 cm ⁻¹ , 60 mW, 50 scans	Rare mineral. Synthetic from 1923	Fig. 14
<i>Barium white</i> barium sulfate, BaSO ₄	454m, 464m, 619w, 633w(sh), 648w, 989vs, 1087vw, 1105vw, 1142w, 1168vw	2 cm ⁻¹ , 80 mW, 1000 scans	Mineral (barytes)	Fig. 15
<i>Chalk (calcite)</i> calcium carbonate, CaCO ₃	156m, 283m, 713m, 1087vs	4 cm ⁻¹ , 80 mW, 2000 scans	Mineral	Fig. 16
<i>Gypsum</i> calcium sulfate dihydrate, CaSO ₄ ·2H ₂ O	179w, 415m, 493w, 619w, 670w, 1009vs, 1136m	4 cm ⁻¹ , 90 mW, 1000 scans	Mineral	Fig. 17
<i>Lead white</i> basic lead(II) carbonate, 2PbCO ₃ ·Pb(OH) ₂	415w(br), 681w, 1051s, 1055s	1 cm ⁻¹ , 160 mW, 100 scans	Rare mineral (hydrocerussite). Synthetic (pre-500 BC)	Fig. 18
<i>Lithopone</i> zinc sulfide and barium sulfate, ZnS and BaSO ₄	348w, 453m, 462m, 617w, 647w, 988vs	1 cm ⁻¹ , 100 mW, 100 scans	1874	Fig. 19
<i>Rutile</i> titanium dioxide, TiO ₂	144w, 232m(br), 447s, 609s	8 cm ⁻¹ , 30 mW, 100 scans	Mineral. Synthetic from 1947	Fig. 20
<i>Zinc white</i> zinc oxide, ZnO	100m, 331w(br), 438vs, 489w(br)	8 cm ⁻¹ , 30 mW, 200 scans	1834	Fig. 21

^a $\pm 1 \text{ cm}^{-1}$.

^b s, strong; m, medium; w, weak; v, very; sh, shoulder; br, broad.

^c Resolution, power at the sample, number of scans.

^d The pigment is either specified to be a mineral or the date of its first manufacture is listed.

Table 4
Yellow pigments analysed with the Bruker FT-Raman spectrometer ($\lambda_0 = 1064 \text{ nm}$)

Name and composition	Band wavenumber ^c /cm ⁻¹ and relative intensity ^d	Experimental details ^c	Notes	Figure
<i>Barium yellow</i> barium chromate, BaCrO ₄	68w, 351m, 361m, 404m, 412w, 428w, 864vs, 873m, 885w, 900m, 907w	1 cm ⁻¹ , 150 mW, 45 scans	Early 19th C. known as <i>lemon yellow</i>	Fig. 22
<i>Berberine</i> ^a [C ₂₀ H ₁₈ N ₁ O ₄] ⁺ plus sulfate or chloride anion	714w, 732w, 754w, 772w, 837w, 979w, 1105vw, 1120vw, 1145vw, 1205m, 1237w, 1278m, 1335w(sh), 1345w, 1365w, 1398vs, 1426m, 1449m, 1501s, 1521vs, 1570m, 1623s, 1636s, 2849w, 2912w, 2954w, 3001w, 3022w, 3074w	4 cm ⁻¹ , 8 mW, 400 scans	Antiquity. Principal chromophore of the <i>huangbo</i> and <i>kihada</i> dyes	Fig. 23
<i>Chrome yellow light</i> lead(II) chromate, PbCrO ₄	141w, 339w, 361s, 378m, 405w, 842s, 864m	1 cm ⁻¹ , 150 mW, 150 scans	Rare mineral crocoite. Synthetic, 1809	Fig. 24
<i>Chrome yellow–orange</i> basic lead(II) chromate, PbCrO ₄ ·PbO	63w, 151m, 341m, 359m, 824s, 844s(sh)	1 cm ⁻¹ , 16 mW, 450 scans	Synthetic, 1809	Fig. 25
<i>Cobalt yellow</i> potassium cobalt(III) nitrite, K ₃ [Co(NO ₂) ₆]·3H ₂ O	111m, 180m, 276m, 305s, 821s, 837m, 1258w, 1327s, 1398w	2 cm ⁻¹ , 30 mW, 150 scans	1861. Also known as aureolin	Fig. 26
<i>Gamboge</i> ^b α - and β -gambogic acids, C ₃₈ H ₄₄ O ₈ and C ₂₉ H ₃₆ O ₆	1224w, 1249m, 1281w, 1333w, 1383w, 1437m, 1594s, 1634m	2 cm ⁻¹ , 55 mW, 800 scans	Before 1640, gum–resin	Fig. 27
<i>Lead tin yellow, type I</i> lead(II) stannate, Pb ₂ SnO ₄	81m, 113w, 131s, 197m, 276w(br), 294w, 459m	2 cm ⁻¹ , 16 mW, 145 scans	Antiquity	Fig. 28
<i>Massicot</i> orthorhombic lead(II) oxide, PbO	72w, 87m, 142vs, 285m	1 cm ⁻¹ , 16 mW, 100 scans	Antiquity	Fig. 29
<i>Mosaic gold</i> tin(IV) sulfide, SnS ₂	314m	8 cm ⁻¹ , 4 mW, 450 scans	Mineral. Synthetic since 13th century	Fig. 30
<i>Naples yellow</i> lead(II) antimonate, Pb ₂ Sb ₂ O ₇	74w, 88w, 144vs, 289m, 342w, 345w, 465w	8 cm ⁻¹ , 6 mW, 100 scans	Synthetic (Egypt, c. 1500 BC)	Fig. 31
<i>Orpiment</i> arsenic(III) sulfide, As ₂ S ₃	70w, 107w, 137w, 155m, 158w(sh), 180w, 183w, 193w, 203m, 221w, 294m, 308s, 312s(sh), 353vs, 356vs(sh), 361s, 369w, 384w	0.5 cm ⁻¹ , 16 mW, 80 scans	Mineral	Fig. 32
<i>Palmatine</i> ^a [C ₂₁ H ₁₈ N ₁ O ₄] ⁺ plus counter-anion	477w, 738m, 1152m, 1193m, 1210m, 1287m, 1339m, 1355m, 1377m, 1395s, 1425m, 1455w, 1449m, 1514s, 1525s(sh), 1570w, 1584m, 1606s, 1637s	8 cm ⁻¹ , 8 mW, 500 scans	Antiquity. Secondary chromophore of <i>huangbo</i> and <i>kihada</i> dyes	Fig. 33

Table 4 (Continued)

Name and composition	Band wavenumber ^c /cm ⁻¹ and relative intensity ^d	Experimental details ^e	Notes	Figure
<i>Pararealgar</i> arsenic(II) sulfide, As ₄ S ₄	118m, 142m, 153m, 158m, 172m, 176m, 191w, 197m, 204m, 230vs, 236s, 275w, 315w, 320w, 333m, 346m, 364m, 371w	0.5 cm ⁻¹ , 8 mW, 500 scans	Light induced transformation product of realgar	Fig. 34
<i>Saffron</i> crocetin, carotenoid dicarboxylic acid, C ₂₀ H ₂₄ O ₄	1020w, 1166m, 1210w, 1283w, 1537s, 1613w	4 cm ⁻¹ , 60 mW, 500 scans	Antiquity. Crocus flower stigma	Fig. 35
<i>Strontium yellow</i> strontium chromate, SrCrO ₄	339w, 348w, 374w, 431vw, 859s, 867vs, 890vs, 895vs, 917m, 931w	1 cm ⁻¹ , 150 mW, 45 scans	Early 1800s	Fig. 36
<i>Turmeric</i> curcumine, C ₂₁ H ₂₀ O ₆	964w, 1171m, 1186m, 1249m, 1312w, 1431w, 1438w, 1602s, 1632s	2 cm ⁻¹ , 16 mW, 5000 scans	Extract from <i>Curcuma</i> plants	Fig. 37

^a From Professor K.R. Seddon, Queen's University of Belfast.

^b From the Tate Gallery, London.

^c ± 1 cm⁻¹.

^d s, strong; m, medium; w, weak; v, very; sh, shoulder; br, broad.

^e Resolution, power at the sample, number of scans.

Table 5
Synthetic pigments post 1860 AD analysed with the Bruker FT-Raman spectrometer ($\lambda_0 = 1064$ nm)

Name and composition	Band wavenumber ^a /cm ⁻¹ and relative intensity ^b	Experimental details ^c	Notes	Figure
<i>Bright red</i> β -naphthol (PR112), C ₂₄ H ₁₆ Cl ₃ N ₃ O ₂	75w, 99w, 149m, 247w, 298w, 347w, 386w, 431w, 442w, 454m, 463m, 528w, 573w, 619m, 681m, 725w, 731w, 746w, 813w, 968w, 989vs, 1063w, 1099w, 1109w, 1162m, 1205w, 1231s, 1244w, 1261w, 1282m, 1332w, 1359s, 1376m, 1393m, 1449w, 1463w, 1484m, 1552m, 1580s, 1607w	2 cm ⁻¹ , 80 mW, 700 scans	1939	Fig. 38
<i>Cadmium red</i> cadmium selenosulfide, CdS·x CdSe	136w, 239m, 335vw(br), 988s	8 cm ⁻¹ , 8 mW, 1000 scans	1907	Fig. 39
<i>Hansa yellow</i> (PY6), C ₁₆ H ₁₃ Cl ₁ N ₄ O ₄	70m, 85m(sh), 95m, 118m, 124m, 158m, 177w, 185w, 212w, 284w, 353w, 386w, 394w, 414w, 617w, 626w, 655m, 742m, 761w, 770w, 785w, 823w, 849w, 953m, 1001m, 1068w, 1111w, 1141s, 1181w, 1192w, 1257m, 1306s, 1325m, 1336m, 1360w, 1386m, 1403w, 1451w, 1491s, 1534w, 1561w(sh), 1568m, 1605s, 1619s, 1672w	2 cm ⁻¹ , 80 mW, 200 scans	1910	Fig. 40
<i>Permanent magenta</i> formula N.A.	91s, 187m, 227m, 309m, 346m, 369w, 460m, 543m, 557m, 679w, 721s, 877w, 951w, 1198m, 1233w, 1314s, 1346m, 1380m, 1514m, 1568s, 1594s, 1648m	4 cm ⁻¹ , 80 mW, 1000 scans	Date N.A.	Fig. 41
<i>Phthalocyanine green</i> Cu(C ₃₂ Cl ₁₆ N ₈)	689vw, 706vw, 742vw, 777vw, 1212w, 1292w, 1341w, 1393vw, 1538m	8 cm ⁻¹ , 3 mW, 300 scans	1936	Fig. 42
<i>Quinacridone violet</i> formula N.A.	416m, 709s, 1309s, 1570s, 1594s, 1649w	4 cm ⁻¹ , 16 mW, 1500 scans	Date N.A.	Fig. 43
<i>Studio red</i> Hansa red formula N.A.	77w, 104w, 125w, 139w, 169w, 197w, 342m, 366w, 384w, 403w, 424w, 457w, 480w, 503m, 514w, 618m, 678w, 724m, 798m, 844m, 925w, 987m, 1077w, 1084w, 1099w, 1129m, 1159w, 1187m, 1217m, 1252w, 1258w, 1282vw, 1309m, 1322s, 1334 vs, 1397m, 1446s, 1482w, 1496m, 1527w, 1556m, 1576w, 1607m, 1622s	2 cm ⁻¹ , 80 mW, 480 scans	Date N.A.	Fig. 44

^a ± 1 cm⁻¹.

^b s, strong; m, medium; w, weak; v, very; sh, shoulder; br, broad.

^c Resolution, power at the sample, number of scans.

Table 6
Miscellaneous materials and minerals analysed with the Bruker FT-Raman spectrometer ($\lambda_0 = 1064 \text{ nm}$)

Name and composition	Band wavenumber ^a /cm ⁻¹ and relative intensity ^b	Experimental details ^c	Notes ^d	Figure
<i>Anhydrite</i> calcium sulfate, CaSO ₄	416m, 498m, 608m, 626m, 675m, 1018s, 1130m, 1161w	8 cm ⁻¹ , 24 mW, 50 scans	Mineral	Fig. 45
<i>Barium carbonate</i> BaCO ₃	137s, 155s, 225w, 962w, 1060s	8 cm ⁻¹ , 16 mW, 100 scans	Mineral	Fig. 46
<i>Indirubin</i> C ₁₆ H ₁₀ N ₂ O ₂	64w, 83m, 114w, 139w, 221w, 269w, 296w, 368w, 382w, 471w, 496w, 532w, 573w, 631w, 669w, 680w, 721w, 782w, 803w, 877w, 890w, 963w, 1008w, 1024w, 1143w, 1153w, 1181w, 1194w, 1215w, 1276w, 1292w, 1320w, 1386w, 1402w, 1464w, 1481w, 1588s, 1619w, 1636w	2 cm ⁻¹ , 24 mW, 100 scans	Plant extract	Fig. 47
<i>Lead(II) carbonate</i> PbCO ₃	57m, 73m, 102m, 150w, 174w, 222w, 668vw, 673vw, 681vw, 694vw, 837vw, 1046m, 1053vs, 1368w(br), 1475w(br)	1 cm ⁻¹ , 100 mW, 200 scans	Mineral (cerussite)	Fig. 48
<i>Lead(II) sulfate</i> PbSO ₄	437m, 449m, 605w, 642w, 979s, 1057w	4 cm ⁻¹ , 4 mW, 100 scans	Mineral	Fig. 49
<i>Magnesium carbonate monohydrate</i> , MgCO ₃ ·H ₂ O	1122w	8 cm ⁻¹ , 16 mW, 200 scans	Mineral	Fig. 50
<i>Magnesium sulfate</i> MgSO ₄	985s	8 cm ⁻¹ , 16 mW, 300 scans	Mineral	Fig. 51
<i>Perspex</i> Polymethylmethacrylate (PMMA)	97m, 300w, 366w, 485w, 558vw(sh), 602w, 813m, 969w, 989w, 1067vw, 1124vw, 1158vw, 1186vw, 1239vw, 1454m, 1490w, 2485w, 2952s, 3002m	8 cm ⁻¹ , 80 mW, 200 scans	Synthetic polymer	Fig. 52
<i>Silica</i> silicon oxide, SiO ₂	130m, 208m, 262vw, 354vw, 398vw, 466s	8 cm ⁻¹ , 100 mW, 300 scans	Mineral	Fig. 53
<i>Sodium carbonate</i> Na ₂ CO ₃	702w, 1071m, 1081vs	2 cm ⁻¹ , 80 mW, 200 scans	Mineral	Fig. 54
<i>Tin(II) chloride dihydrate</i> SnCl ₂ ·2H ₂ O	118m, 130m, 193w(br), 276w, 318w, 353s, 435w	2 cm ⁻¹ , 16 mW, 200 scans	Mineral	Fig. 55

^a $\pm 1 \text{ cm}^{-1}$.

^b s, strong; m, medium; w, weak; v, very; sh, shoulder; br, broad.

^c Resolution, power at the sample, number of scans.

^d The pigment is either specified to be a mineral or the date of its first manufacture is listed.

Table 7

Binding media and varnishes analysed with the Bruker FT-Raman spectrometer ($\lambda_0 = 1064$ nm)

Name and composition	Band wavenumber ^b /cm ⁻¹ and relative intensity ^c	Experimental details ^d	Notes ^e	Figure
<i>Bees wax</i> ^a mainly myricyl palmitate ester, C ₁₅ H ₃₁ CO ₂ C ₃₀ H ₆₁	891vw, 1062w, 1129w, 1295m, 1369w, 1418m, 1440m, 1460w, 2723w, 2849s, 2881vs	8 cm ⁻¹ , 130 mW, 100 scans	Wax of insect origin	Fig. 56
<i>Egg white</i> ^a	1004w, 1451w, 1666w, 2728vw, 2874m, 2932vs, 3059w	8 cm ⁻¹ , 130 mW, 100 scans	Protein mixture	Fig. 57
<i>Egg yolk</i> ^a	865w(br), 1075w, 1304m, 1446m, 1661w, 2730w, 2854vs, 2898vs, 2933vs	8 cm ⁻¹ , 130 mW, 100 scans	Protein mixture	Fig. 58
<i>Gum arabic</i>	458vw, 844w, 883w, 965w, 1028w(sh), 1083m, 1269w, 1346w, 1372w(sh), 1419w, 1461w, 2926s	8 cm ⁻¹ , 80 mW, 500 scans	Acacia shrub or tree resin	Fig. 59
<i>Linseed oil</i> ^a	865w(br), 1076w(br), 1302m, 1443m, 1658w, 1744w, 2855vs, 2909vs	8 cm ⁻¹ , 130 mW, 100 scans	Oil obtained from flax seeds	Fig. 60

^a Donated by Dr D. Bikiaris, University of Thessaloniki, Greece.

^b ± 1 cm⁻¹.

^c s, strong; m, medium; w, weak; v, very; sh, shoulder; br, broad.

^d Resolution, power at the sample, number of scans.

^e The pigment is a natural plant or animal product.

The reference materials which have been analysed by FT-Raman spectroscopy have been divided into three groups; the first contains most of the pigments [24–30], both natural and synthetic, that were in use before the isolation of the first organic dye by Perkin in 1856. These pigments have been arranged in different tables alphabetically according to their colours (Tables 1–4). The second group of reference materials contains a restricted number of organic pigments synthesised after 1856 (Table 5). The third group (Tables 6 and 7) contains a number of organic and inorganic materials, such as minerals, binding media and varnishes, which are not pigments, but which are likely to be found on works of art. Table 8 indicates those pigments for which it was either extraordinarily difficult or impossible to obtain a Raman spectrum with 1064 nm excitation.

Raman spectra recorded using visible excitation have also been collected in this study for reference purposes. The spectra presented here include those of a number of pigments and minerals, those of pigments being arranged alphabetically

by colour (Tables 9–11) and those of the minerals and other materials being listed in a separate table (Table 12).

This paper thus consists of the Raman spectra of over 80 pigments, minerals and binders [31] and can be considered to be a supplement to the Raman spectroscopic library published in 1997 by Bell et al. and involving visible excitation only [23]. In the present paper a larger number of materials has been analysed and a wider range of experimental conditions employed; for example, the Raman spectrometers used to collect the spectra presented here have holographic notch filters which allow the detection of Raman bands down to 50 rather than 100 cm⁻¹. Some of the FT-Raman experiments which have provided the main data for this paper yielded spectra at relatively high resolution (down to 0.5 cm⁻¹). Also, some Raman spectra collected with the Dilor XY spectrometer have been included in this collection, allowing the detection of bands below 50 cm⁻¹. In a few cases relatively poor FT-Raman spectra have been included in the collection. They represent the best spectra which could be obtained by

the authors using the instrumentation specified [22], and are shown as examples of what could be expected in experiments on artworks.

2. Experimental

A Bruker RFS 100/S FT-Raman microscope was used to collect all the FT-Raman spectra, the instrument being equipped with a Nikon microscope and a Nd:YAG c.w. laser operating at 1064 nm. The powers used in the experiments performed with this instrument were much higher than those needed with a Raman microscope operating in the visible region. The minimum setting suggested by the manufacturer corresponded to 4 mW at the sample. However, satisfactory results could be

achieved using ~ 2 mW. The maximum power available was ~ 300 mW.

The visible Raman spectra were collected using the following spectrometers:

- a Dilor XY Raman microscope, a triple-grating spectrometer configured with an Olympus BH-2 microscope and a photodiode array detector operating at -38 °C. The excitation source was a water-cooled Coherent I301 1 W krypton ion laser operating at 647.1 nm;
- a Renishaw Raman System 1000 instrument at the Raman Laboratory, UCL, configured with a Nikon microscope and a Renishaw slow-scan CCD camera thermoelectrically cooled to -70 °C. The excitation sources were a Spectra-Physics argon ion laser operating at 514.5 nm and a Renishaw He–Ne laser operating at 632.8 nm;

Table 8
Pigments with no detectable Raman signal using 1064 nm excitation

Colour	Name and composition	Notes
Black	Ivory black, carbon	Antiquity
	Lamp black, carbon	Antiquity
	Plattnerite, lead(IV) oxide, PbO ₂	Mineral
	Galena, lead(II) sulfide, PbS	Mineral
Blue	Prussian blue, iron(III) hexacyanoferrate(II), Fe ₄ [Fe(CN) ₆] ₃ ·14-16H ₂ O	1704
	Cobalt blue, cobalt(II)-doped alumina glass, CoO·Al ₂ O ₃	1775
	Cerulean blue, cobalt(II) stannate, CoO·nSnO ₂	1821
Green	Malachite, basic copper(II) carbonate, CuCO ₃ ·Cu(OH) ₂	Mineral
	Copper(II) chloride, CuCl ₂	Mineral
	Tutton salt, hydrated ammonium copper(II) sulfate (NH ₄) ₂ Cu(SO ₄) ₂ ·6H ₂ O	Mineral
	Cu(II) oxalate dihydrate, CuC ₂ O ₄ ·2H ₂ O	Mineral
	Atacamite, basic copper(II) chloride, CuCl ₂ ·3Cu(OH) ₂	Mineral
	Emerald green, copper(II) ethanoate tri-copper(II) arsenite, Cu[C ₂ H ₃ O ₂] ₃ ·3Cu[AsO ₂] ₂	1814
	Brochantite, basic copper(II) sulfate Cu ₄ (OH) ₆ SO ₄	Mineral
	Green earth, variations on K[(Al ^{III} , Fe ^{III})(Fe ^{II} , Mg ^{II})] ₂ (AlSi ₃ Si ₄)O ₁₀ (OH) ₂	Mineral
	Chromium(III) oxide, Cr ₂ O ₃	Early 1800s
	Viridian, hydrated chromium(III) oxide, Cr ₂ O ₃ ·2H ₂ O	1838 (?1850)
Red	Verdigris, copper(II) ethanoate, Cu(CH ₃ COO) ₂	Synthetic (BC)
	Cobalt green, cobalt(II) zincate, CaO·nZnO	1780
	Scheele's green, copper(II) arsenite, Cu(AsO ₂) ₂	1778
	Cuprite, copper(I) oxide, Cu ₂ O	Mineral
Yellow	Purpurin (chromophore, with alizarin, in the madder dye), 1,2,4-trihydroxy-anthraquinone, C ₁₄ H ₁₈ O ₅	3000 BC
	Cadmium yellow, cadmium(II) sulfide, CdS	Mineral, synthetic ca. 1845
	Mars yellow, synthetic iron(III) oxide hydrated	Middle 19th century

Table 9
Green pigments analysed using visible excitation

Name and composition	Band wavenumber ^a /cm ⁻¹ and relative intensity ^b	Experimental details ^c	Notes ^d	Figure
<i>Atacamite</i> orthorhombic basic copper(II) chloride, Cu ₂ (OH) ₃ Cl	106w, 121s, 361m(br), 419w(br), 446w, 475w, 511s, 818m(br), 846w, 912s, 975s	514.5 nm, 2 cm ⁻¹ , 0.5 mW, 50 scans (10 s)	Mineral	Fig. 61
<i>Brochantite</i> basic copper(II) sulfate, Cu ₄ (OH) ₆ SO ₄	90w, 104vw, 118vw, 123w, 130vw, 139w, 149vw, 156vw, 169vw, 176vw, 187vw, 196w, 242vw, 318vw, 365vw, 390w, 421w, 450w, 481w, 508vw, 595w, 609w, 620vw, 730vw, 873vw, 912vw, 973s, 1077vw, 1097vw, 1106vw(sh), 1125vw, 3225w, 3258w(br), 3371s, 3399s, 3470w(br), 3564s, 3587 vs	514.5 nm, 2 cm ⁻¹ , 0.5 mW, 45 scans (10 s)	Mineral	Fig. 62
<i>Copper(II) chloride</i> CuCl ₂	95w, 106w, 118s, 140s, 149m(sh), 213m, 362m, 416w, 477w, 511s, 575w, 799w, 819m, 845w, 869w, 893m, 910m, 928m, 971m	514.5 nm, 2 cm ⁻¹ , 0.5 mW, 40 scans (10 s)	Mineral	Fig. 63
<i>Copper(II) oxalate dihydrate</i> CuC ₂ O ₄ ·2H ₂ O	210m, 299vw, 559s, 586m, 611w, 832m, 923m, 1487m, 1516s, 1616w, ~1665vw	514.5 nm, 2 cm ⁻¹ , 0.5 mW, 40 scans (10 s)	Mineral	Fig. 64
<i>Paratacamite</i> rhombohedral basic copper(II) chloride, Cu ₂ (OH) ₃ Cl	95w, 117s, 140s, 165w, 364m, 420w, 511s, 576w, 799w, 868w, 892m, 928m, 970m, 3311s, 3355s, 3441s	514.5 nm, 2 cm ⁻¹ , 0.5 mW, 50 scans (10 s)	Mineral	Fig. 65
<i>Phthalocyanine green</i> Cu(C ₃₂ Cl ₁₆ N ₈)	147w, 164w, 234w, 509w, 642w, 684vs, 739vw, 772vw, 817m, 978vw, 1080s, 1199m, 1210m, 1280m, 1302m, 1338w, 1387s, 1444w, 1478m, 1503vs, 1537s, 1559s	514.5 nm, 2 cm ⁻¹ , 0.5 mW, 15 scans (10 s)	Synthetic (1936)	Fig. 66
<i>Pseudomalachite</i> basic copper(II) phosphate, Cu ₃ (PO ₄) ₂ (OH) ₄	88w, 110m, 131w, 176w, 368w, 450w, 480m, 537w, 609w, 972w, 1000w, 1086m	514.5 nm, 2 cm ⁻¹ , 0.5 mW, 30 scans (10 s)	Mineral	Fig. 67
<i>Tutton salt</i> ammonium copper(II) sulfate hydrate, (NH ₄) ₂ Cu(SO ₄) ₂ ·6H ₂ O	453w, 610vw, 628vw, 982 vs	514.5 nm, 2 cm ⁻¹ , 0.5 mW, 40 scans (10 s)	Mineral	Fig. 68

^a ± 1 cm⁻¹.

^b s, strong; m, medium; w, weak; v, very; sh, shoulder; br, broad.

^c Excitation wavelength, resolution, power at the sample, number of scans (duration of each scan).

^d The pigment is either specified to be a mineral or the date of its first manufacture is listed.

Table 10
Red and blue pigments analysed using visible excitation

Name and composition	Band wavenumber ^a /cm ⁻¹ and relative intensity ^b	Experimental details ^c	Notes ^d	Figure
<i>Carminic acid</i> C ₂₂ H ₂₀ O ₁₃	375w, 434m, 453m, 520w, 554w, 687w, 958w, 1003w, 1076w, 1091w, 1149w, 1225m, 1296m, 1460m, 1572w, 1636w	780.0 nm, 5 mW, 2 cm ⁻¹ , 30 scans (10 s)	Main constituent of red pigment carmine	Fig. 69
<i>Cuprite</i> copper(I) oxide, Cu ₂ O	146m, 217w(br), 242w(br)	632.8 nm, 2 cm ⁻¹ , 0.2 mW, 15 scans (10 s)	Mineral	Fig. 70
<i>Indigo</i> indigotin, C ₁₆ H ₁₀ N ₂ O ₂	182vw, 236w, 253m, 265w, 277w, 311w, 546m, 599m, 635w(br), 676w, 758w, 861vw, 870vw, 1015w, 1126vw, 1148vw, 1226w, 1248w, 1311m, 1363w, 1461w, 1483w, 1572vs, 1584s	780 cm ⁻¹ , 1 mW, 4 scans (10 s)	Extract from plant leaf (BC)	Fig. 71
<i>Phthalocyanine blue</i> CuC ₃₂ H ₁₆ N ₈	166w(br), 173w, 233w, 255w, 592m, 681m, 747w, 777w, 841w, 952w, 1007w, 1037w, 1106w, 1126w, 1339w, 1450m, 1470w, 1482w, 1527s, 1591w, 1610w	514.5 nm, 2 cm ⁻¹ , 1 mW, 10 scans (10 s)	Synthetic (1936)	Fig. 72
<i>Red lead</i> lead(II,IV) oxide, Pb ₃ O ₄	54w, 65w, 86vw, 122vs, 152w, 225vw, 313vw, 391w, 549s	647.1 nm, 2 cm ⁻¹ , 1 mW, 10 scans (3 s)	Antiquity	Fig. 73
<i>Vermilion</i> mercury(II) sulfide, α-HgS	42vs, 253vs, 284w, 343m	647.1 nm, 2 cm ⁻¹ , 1 mW, 5 scans (1 s)	Mineral (cinnabar) and synthetic (8th C)	Fig. 74

^a ± 1 cm⁻¹.

^b s, strong; m, medium; w, weak; v, very; sh, shoulder; br, broad.

^c Wavelength, resolution, power at the sample, number of scans and (duration).

^d The pigment is either specified to be a mineral or the date of its first manufacture is listed.

Table 11
Yellow pigments analysed using visible excitation

Name and composition	Band wavenumber ^a /cm ⁻¹ and relative intensity ^b	Experimental details ^c	Notes ^d	Figure
<i>Litharge</i> tetragonal lead(II) oxide, PbO	82m, 147vs, 339w(br)	647.1 nm, 2 cm ⁻¹ , 1 mW, 10 scans (5 s)	Antiquity	Fig. 75
<i>Massicot</i> orthorhombic lead(II) oxide, PbO	52vw, 77w, 88m, 143vs, 289s, 385w	647.1 nm, 2 cm ⁻¹ , 1 mW, 10 scans (2 s)	Antiquity	Fig. 76
<i>Nickel titanium yellow</i> (Ti, Ni, Sb)O ₂ : crystalline matrix of rutile formed by calcination of titanium oxide, nickel oxide and antimony oxide	130 m(br), 244 m(br), 440s, 615s, 684w(br)	632.8 nm, 2 cm ⁻¹ , 0.5 mW, 10 scans (10 s)	1960s	Fig. 77
<i>Zinc yellow</i> zinc(I) chromate, ZnCrO ₄	112vw, 141vw, 343m, 358w, 410w, 774w, 872s, 893m, 941m	632.8 nm, 2 cm ⁻¹ , 0.5 mW, 10 scans (10 s)	Synthetic (19th C)	Fig. 78

^a ± 1 cm⁻¹.

^b s, strong; m, medium; w, weak; v, very; sh, shoulder; br, broad.

^c Wavelength, resolution, power at the sample, number of scans and (duration).

^d The pigment is either specified to be a mineral or the date of its first manufacture is listed.

Table 12
Miscellaneous materials analysed using visible excitation

Name and composition	Band wavenumber ^a /cm ⁻¹ and relative intensity ^b	Experimental details ^c	Notes ^d	Figure
Graphite C _n	1315w(br), 1579vs	780.0 nm, 2 cm ⁻¹ , 5 mW, 10 scans (10 s)	Mineral (black)	Fig. 79
Haematite Fe ₂ O ₃	224s, 243w, 290s, 299s(sh), 408m, 495w, 609w	632.8 nm, 2 mW, 2 cm ⁻¹ , 10 scans (4 s)	Mineral, synthetic (antiquity); also corrosion product	Fig. 80
Lead(II) sulfate PbSO ₄	60w, 97w(br), 133 w(br), 438m, 449m, 605w, 618vw(sh), 641w, 977s, 1059w, 1156w	514.5 nm, 3.8 mW, 2 cm ⁻¹ , 4 scans (10 s)	Mineral (Anglesite)	Fig. 81
Plattnerite lead(IV) oxide, PbO ₂	515vw(br), 540vw(br)	632.8 nm, 0.5 mW, 2 cm ⁻¹ , 10 scans (5 s)	Black mineral; also degradation product of lead compounds	Fig. 82

^a ± 1 cm⁻¹.

^b s, strong; m, medium; w, weak; v, very; sh, shoulder; br, broad.

^c Wavelength, resolution, power at the sample, number of scans and (duration).

^d The pigment is either specified to be a mineral or the date of its first manufacture is listed.

● a Renishaw instrument at LGC, Teddington, configured with a Nikon microscope and a Renishaw slow-scan CCD camera thermoelectrically cooled to -70 °C. It was equipped with a GaAlAs diode laser operating at 780.0 nm.

In a typical experiment the laser was focused onto the sample through a microscope objective. Depending on the instrument used the laser power at the sample was between 0.01 and 35 mW, controlled with the aid of suitable neutral density filters (Melles Griot). The lowest available power was invariably used first, in order to avoid any possible photo-degradation of the sample.

Wavenumber calibration was achieved by the superposition of neon or mercury emission lines onto the spectra. In selected cases the plasma lines of the Ar ion laser were also used. A linear calibration curve was found to be adequate for most spectra. The resulting calibration corrections were usually slightly less than ± 1 cm⁻¹ but, for consistency, all values reported here are rounded to the nearest integer and so have an estimated uncertainty of ± 1 cm⁻¹. Higher uncertainties, however, must be placed on bands described as broad (br) or shoulders (sh) in the tables of band wavenumbers. The intensities have not been corrected for the spectral response of each instrument. Unless otherwise indicated, all materials have been

analysed with a $\times 50$ microscope objective. The pigments analysed belong to the UCL Raman laboratory collection; most of them were originally purchased from Kremer Pigmente, some are specific donations (see the tables), and some are of unknown provenance. The Raman spectra were analysed using the Origin 5.0 software package.

3. Results and discussion

The spectra are illustrated in Figs. 1–82 and they have been grouped as described in Section 1. The

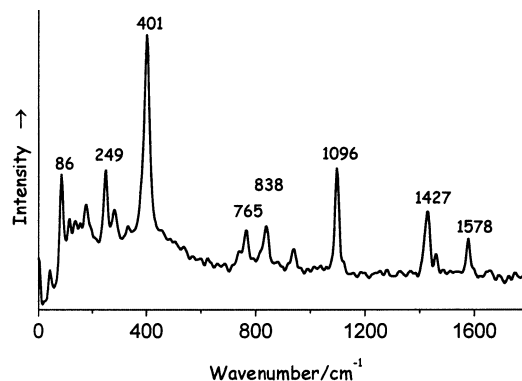
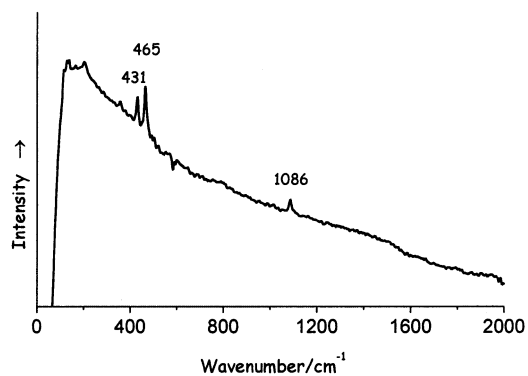
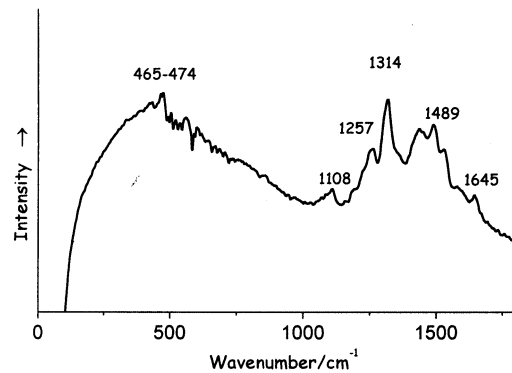
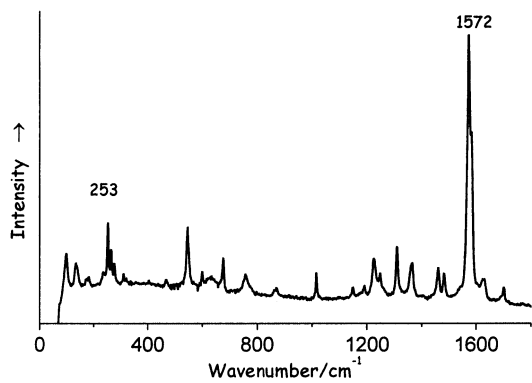
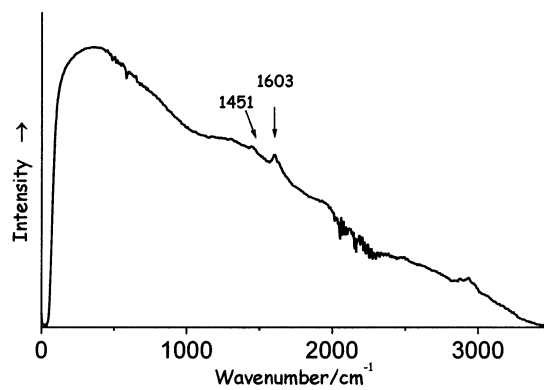
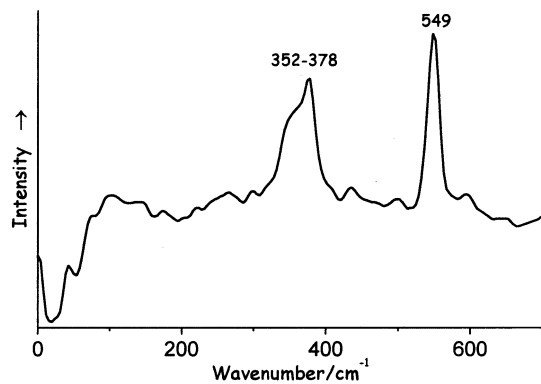
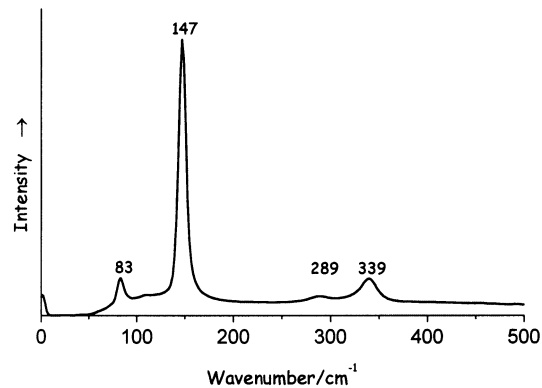
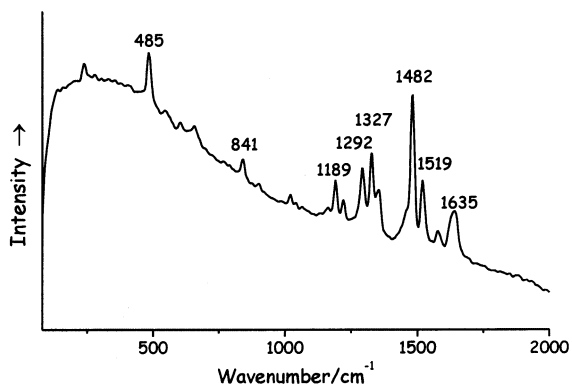
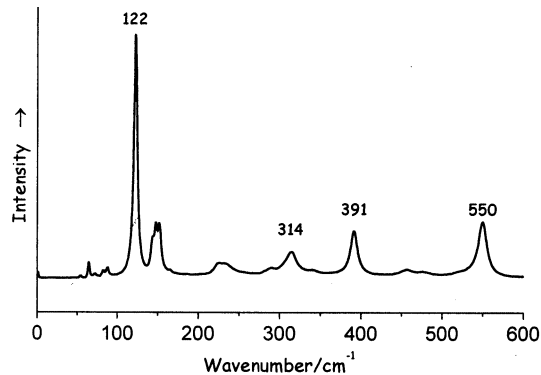
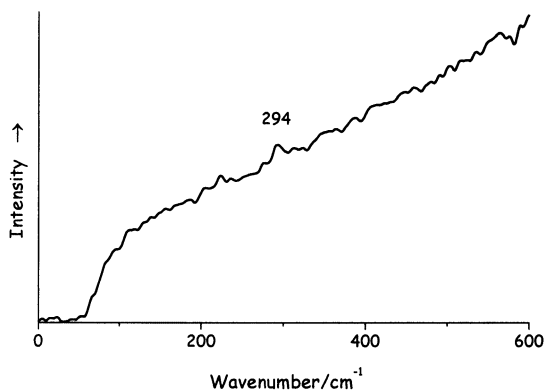
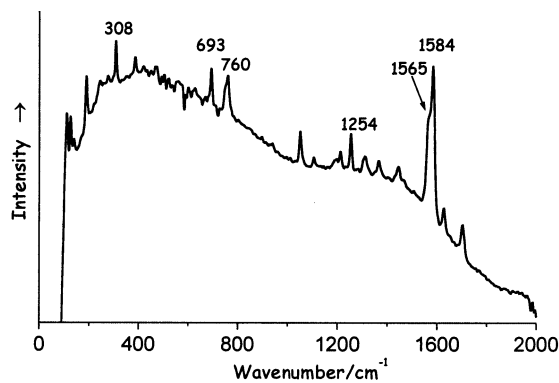
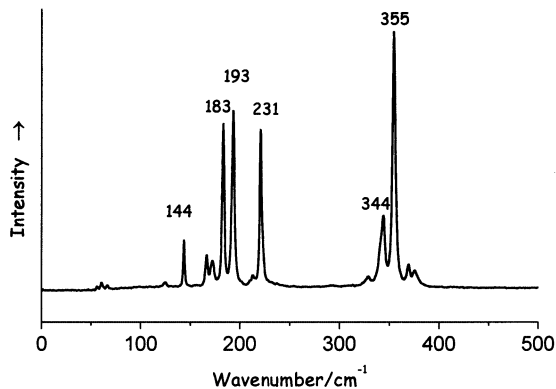
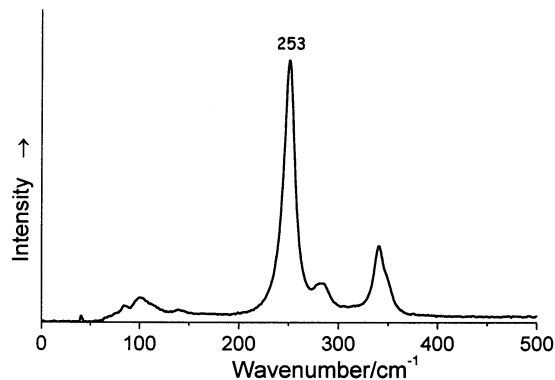
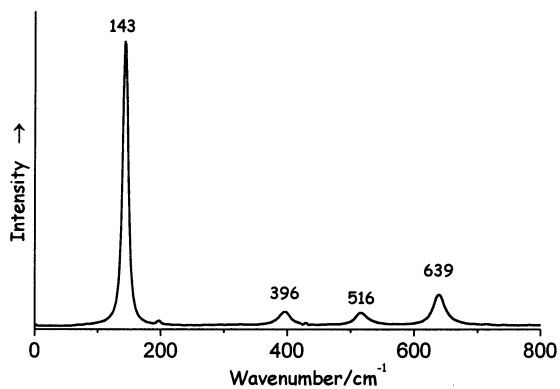
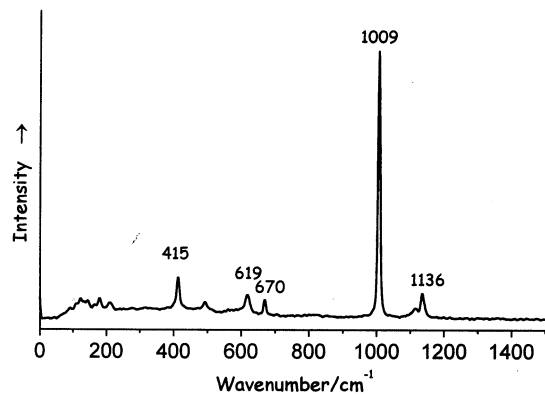
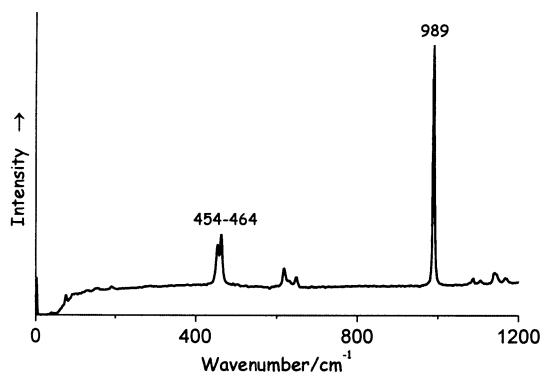
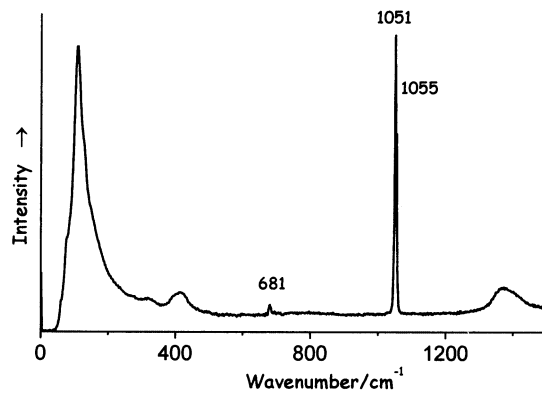
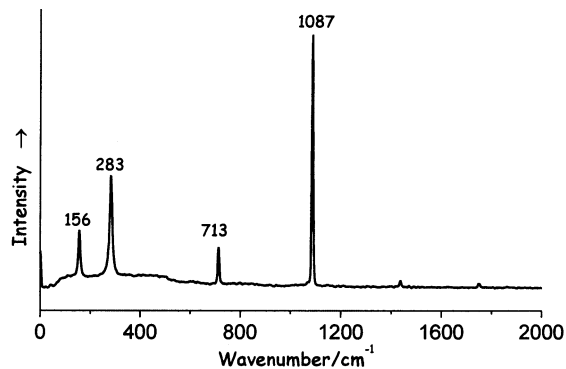
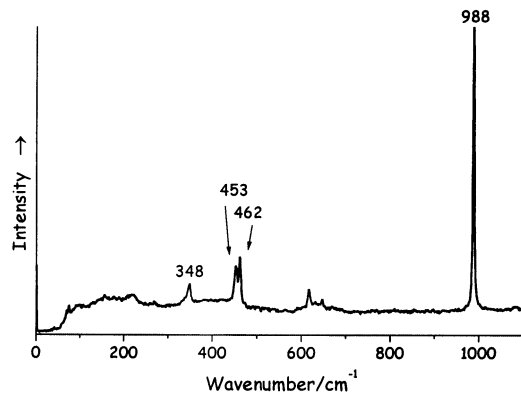
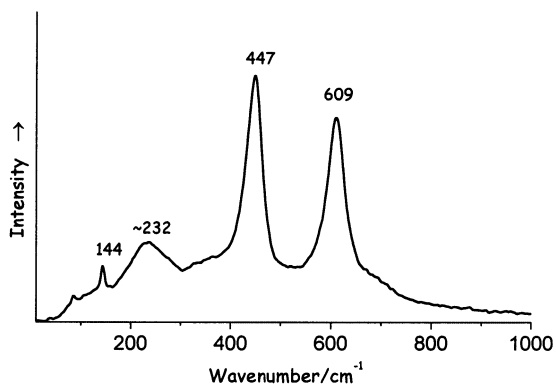
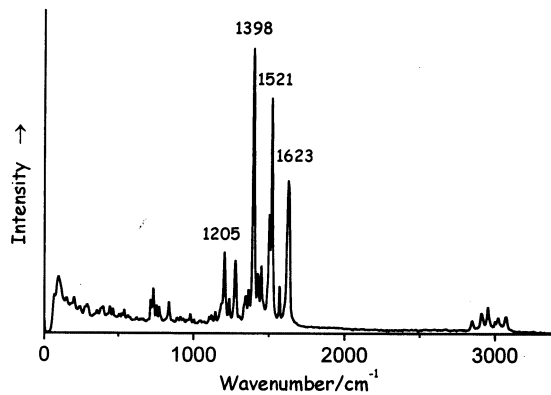
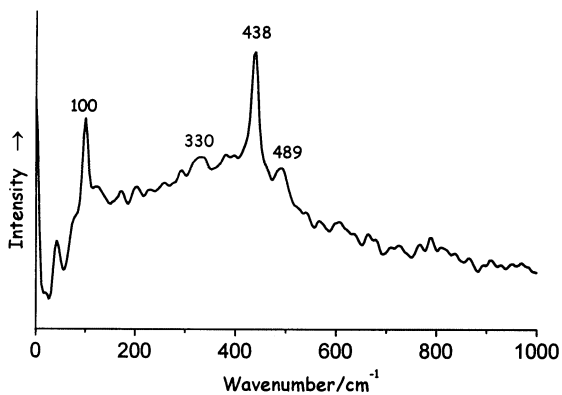
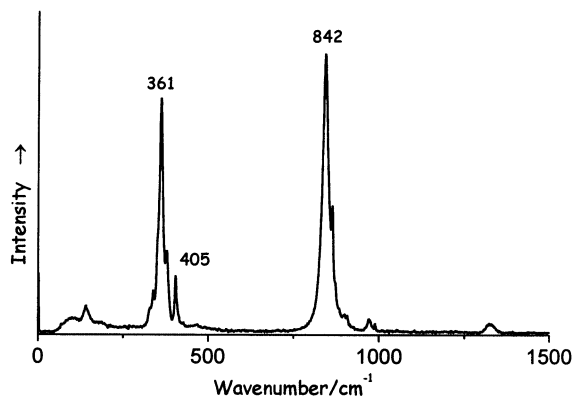
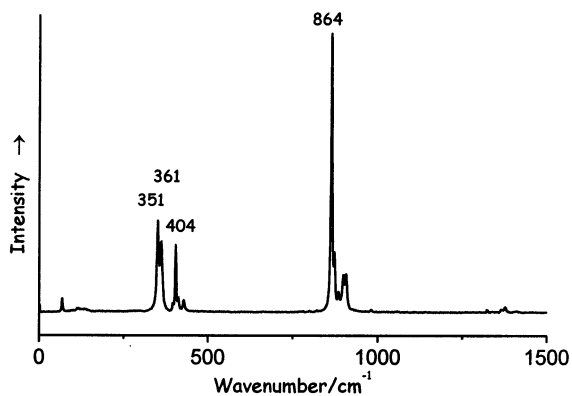
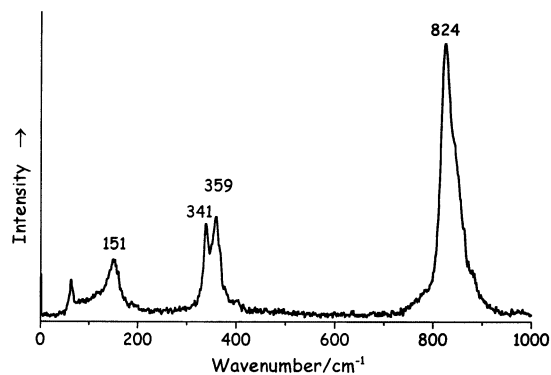


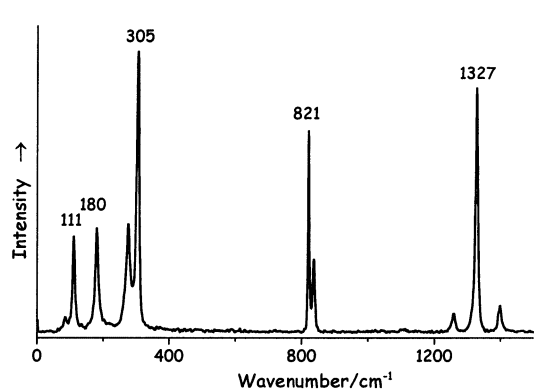
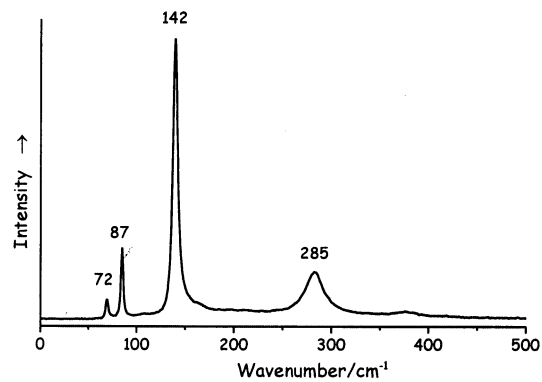
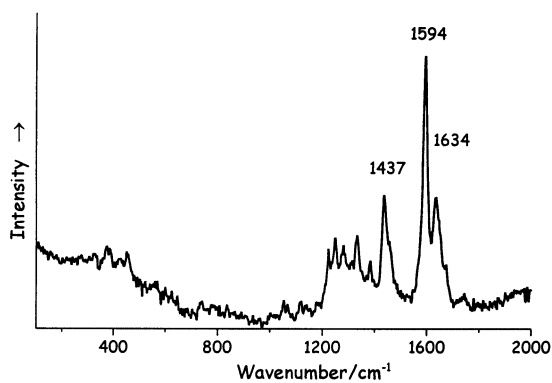
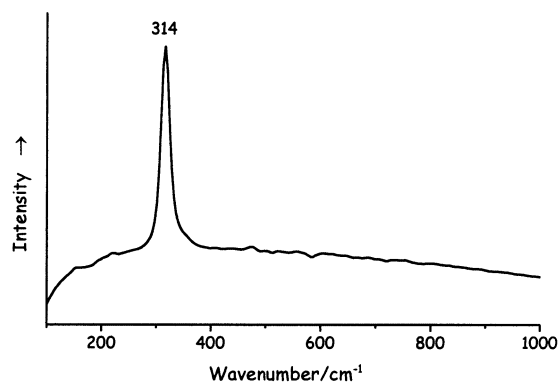
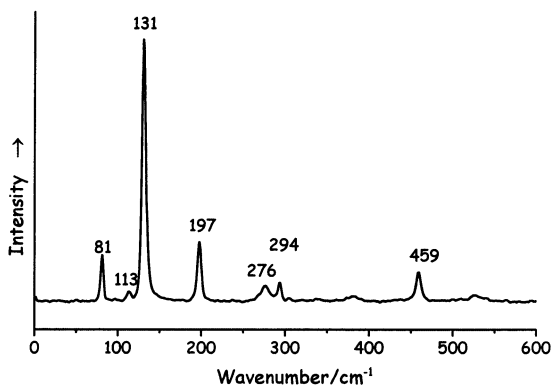
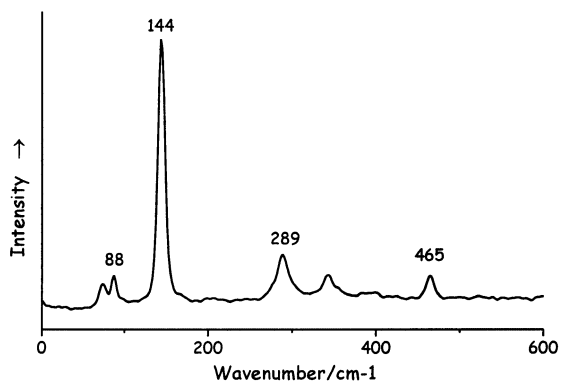
Fig. 1. Azurite, $\lambda_0 = 1064$ nm, 16 mW.

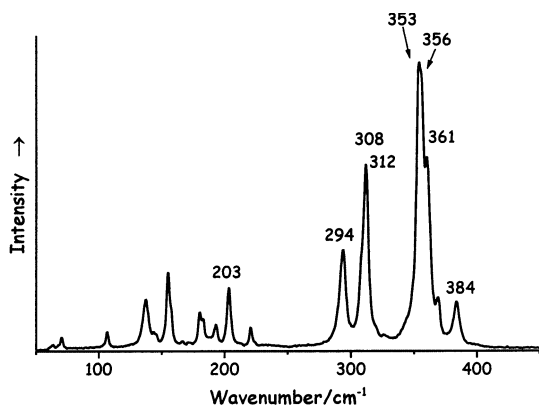
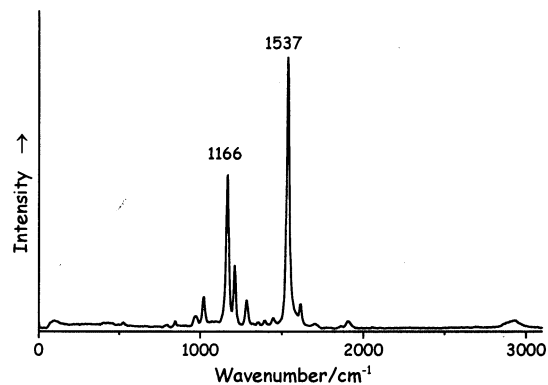
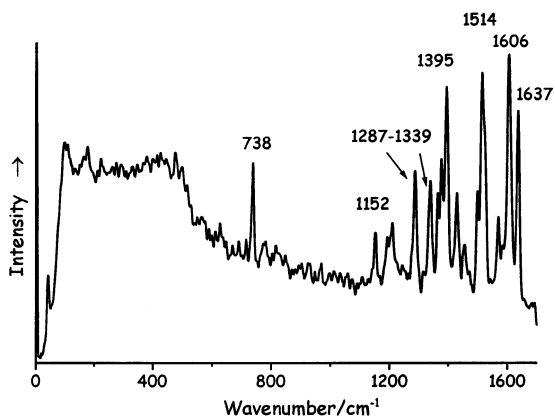
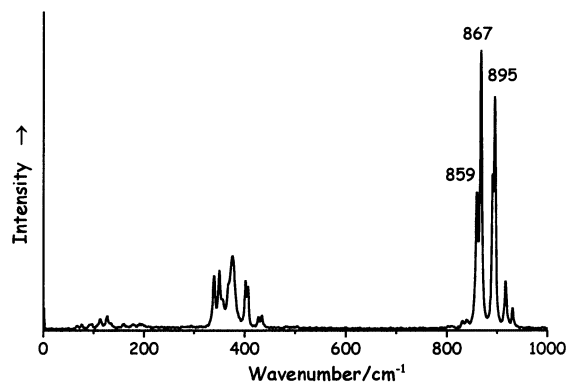
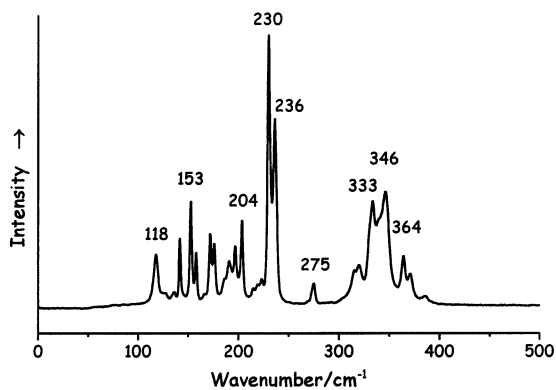
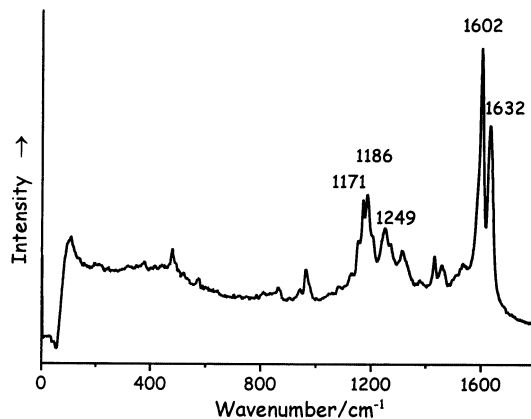
Fig. 2. Egyptian blue, $\lambda_0 = 1064$ nm, 3 mW.Fig. 5. Carmine, $\lambda_0 = 1064$ nm, 16 mW.Fig. 3. Indigo, $\lambda_0 = 1064$ nm, 60 mW.Fig. 6. Kermes, $\lambda_0 = 1064$ nm, 16 mW.Fig. 4. Lazurite, $\lambda_0 = 1064$ nm, 30 mW.Fig. 7. Litharge, $\lambda_0 = 1064$ nm, 270 mW.

Fig. 8. Madder, $\lambda_0 = 1064$ nm, 30 mW.Fig. 11. Red lead, $\lambda_0 = 1064$ nm, 14 mW.Fig. 9. Mars red, $\lambda_0 = 1064$ nm, 4 mW.Fig. 12. Tyrian purple, $\lambda_0 = 1064$ nm, 8 mW.Fig. 10. Realgar, $\lambda_0 = 1064$ nm, 8 mW.Fig. 13. Vermilion, $\lambda_0 = 1064$ nm, 8 mW.

Fig. 14. Anatase, $\lambda_0 = 1064$ nm, 60 mW.Fig. 17. Gypsum, $\lambda_0 = 1064$ nm, 90 mW.Fig. 15. Barium white, $\lambda_0 = 1064$ nm, 100 mW.Fig. 18. Lead white, $\lambda_0 = 1064$ nm, 160 mW.Fig. 16. Calcite, $\lambda_0 = 1064$ nm, 80 mW.Fig. 19. Lithopone, $\lambda_0 = 1064$ nm, 100 mW.

Fig. 20. Rutile, $\lambda_0 = 1064$ nm, 30 mW.Fig. 23. Berberine, $\lambda_0 = 1064$ nm, 8 mW.Fig. 21. Zinc white, $\lambda_0 = 1064$ nm, 30 mW.Fig. 24. Chrome yellow light, $\lambda_0 = 1064$ nm, 150 mW.Fig. 22. Barium yellow, $\lambda_0 = 1064$ nm, 150 mW.Fig. 25. Chrome yellow orange, $\lambda_0 = 1064$ nm, 16 mW.

Fig. 26. Cobalt yellow, $\lambda_0 = 1064$ nm, 30 mW.Fig. 29. Massicot, $\lambda_0 = 1064$ nm, 16 mW.Fig. 27. Gamboge, $\lambda_0 = 1064$ nm, 55 mW.Fig. 30. Mosaic gold, $\lambda_0 = 1064$ nm, 4 mW.Fig. 28. Lead tin yellow (I), $\lambda_0 = 1064$ nm, 16 mW.Fig. 31. Naples yellow, $\lambda_0 = 1064$ nm, 6 mW.

Fig. 32. Orpiment, $\lambda_0 = 1064$ nm, 16 mW.Fig. 35. Saffron, $\lambda_0 = 1064$ nm, 60 mW.Fig. 33. Palmatine, $\lambda_0 = 1064$ nm, 8 mW.Fig. 36. Strontium yellow, $\lambda_0 = 1064$ nm, 150 mW.Fig. 34. Pararealgar, $\lambda_0 = 1064$ nm, 8 mW.Fig. 37. Turmeric, $\lambda_0 = 1064$ nm, 16 mW.

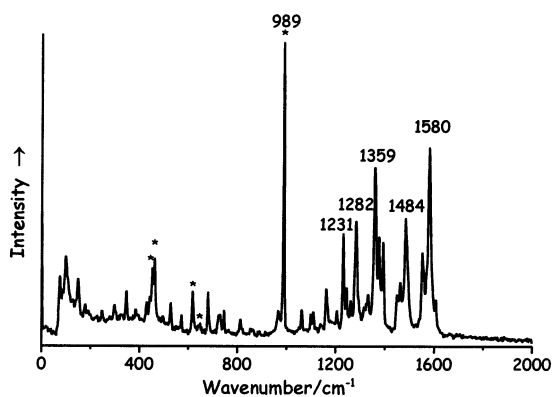


Fig. 38. Bright red, $\lambda_0 = 1064$ nm, 80 mW. (The asterisks mark the bands due to the filler, barium sulfate).

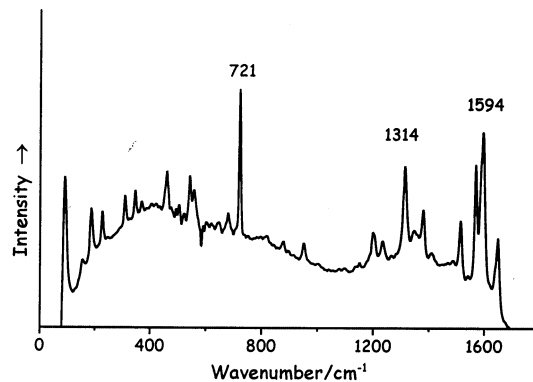


Fig. 41. Permanent magenta, $\lambda_0 = 1064$ nm, 80 mW.

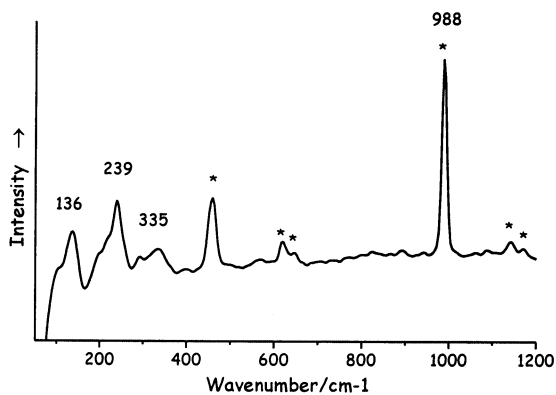


Fig. 39. Cadmium red, $\lambda_0 = 1064$ nm, 8 mW. (The asterisks mark the bands due to the filler, barium sulfate).

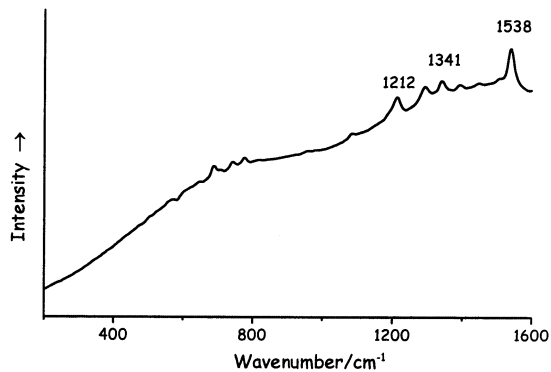


Fig. 42. Phthalocyanine green, $\lambda_0 = 1064$ nm, 3 mW.

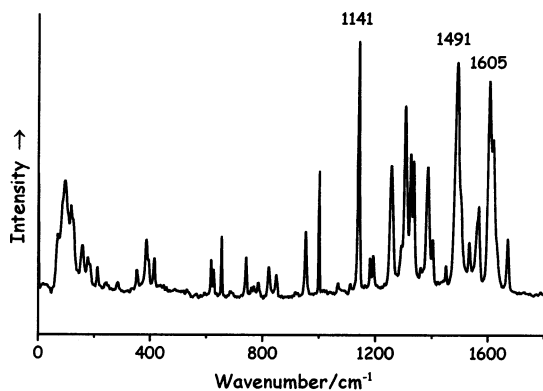


Fig. 40. Hansa Yellow PY6, $\lambda_0 = 1064$ nm, 80 mW.

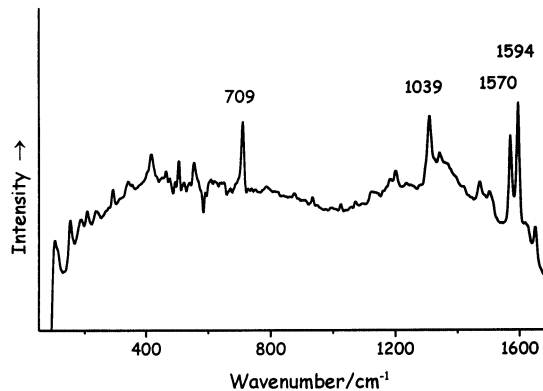
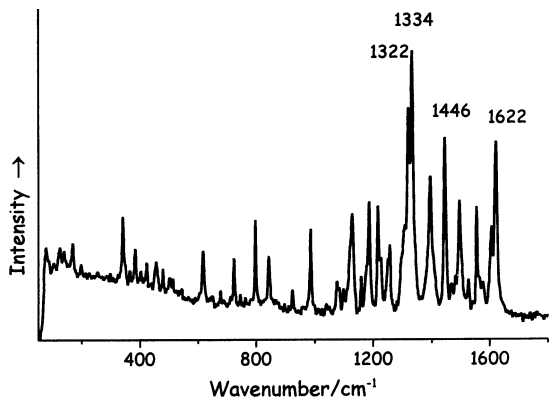
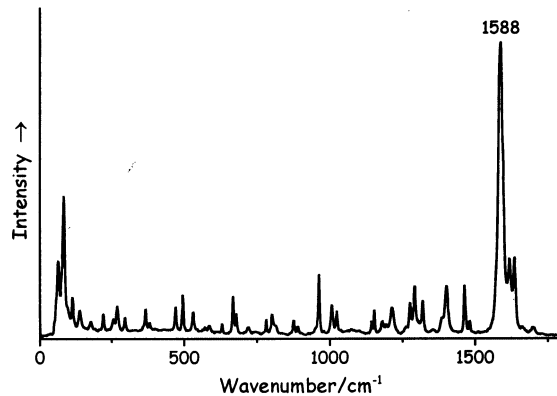
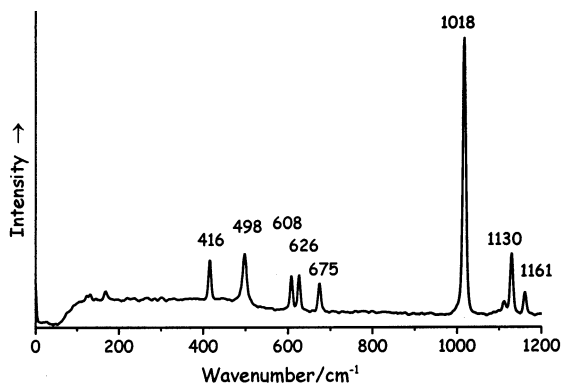
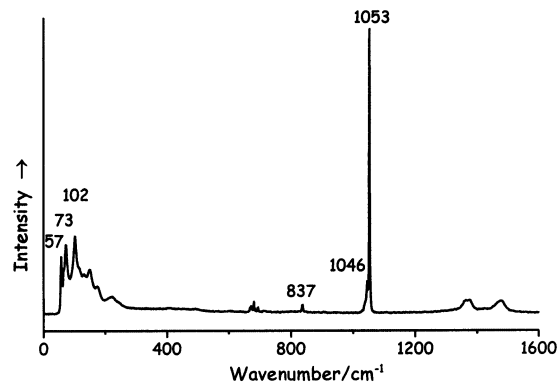
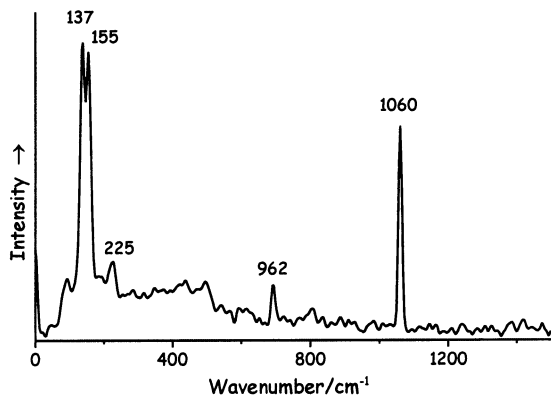
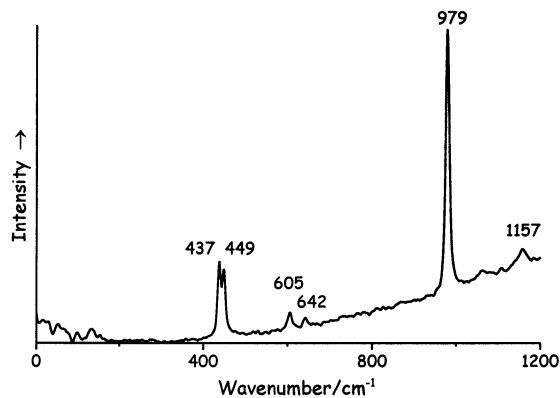


Fig. 43. Quinacridone violet, $\lambda_0 = 1064$ nm, 16 mW.

Fig. 44. Studio red, $\lambda_0 = 1064$ nm, 80 mW.Fig. 47. Indirubin, $\lambda_0 = 1064$ nm, 24 mW.Fig. 45. Anhydrite, $\lambda_0 = 1064$ nm, 24 mW.Fig. 48. Lead carbonate, $\lambda_0 = 1064$ nm, 100 mW.Fig. 46. Barium carbonate, $\lambda_0 = 1064$ nm, 16 mW.Fig. 49. Lead sulfate, $\lambda_0 = 1064$ nm, 4 mW.

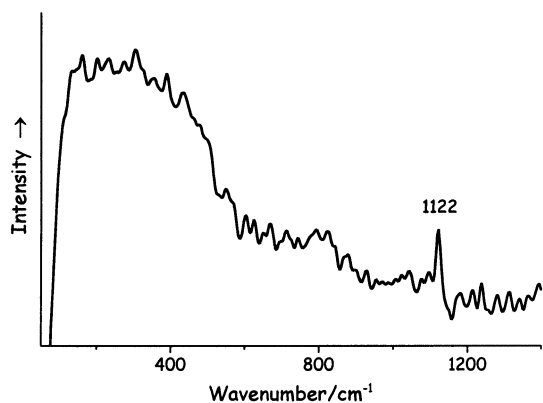


Fig. 50. Magnesium carbonate monohydrate, $\lambda_0 = 1064$ nm, 16 mW.

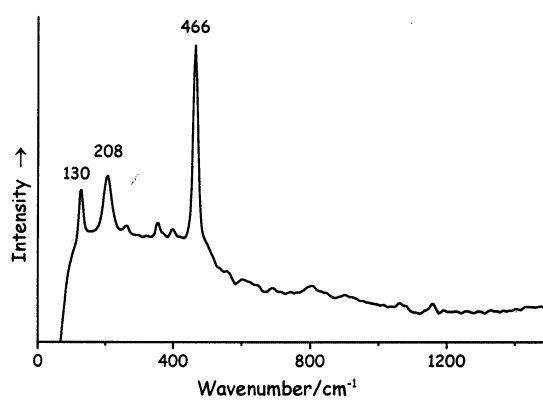


Fig. 53. Silica, $\lambda_0 = 1064$ nm, 100 mW.

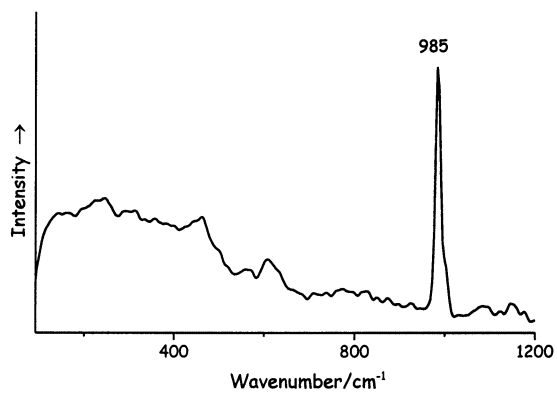


Fig. 51. Magnesium sulfate, $\lambda_0 = 1064$ nm, 16 mW.

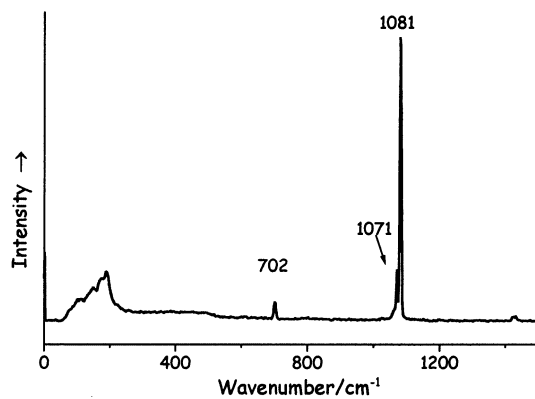


Fig. 54. Sodium carbonate, $\lambda_0 = 1064$ nm, 80 mW.

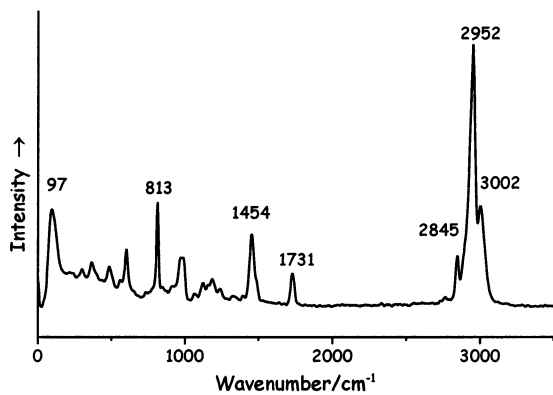


Fig. 52. Perspex, $\lambda_0 = 1064$ nm, 80 mW.

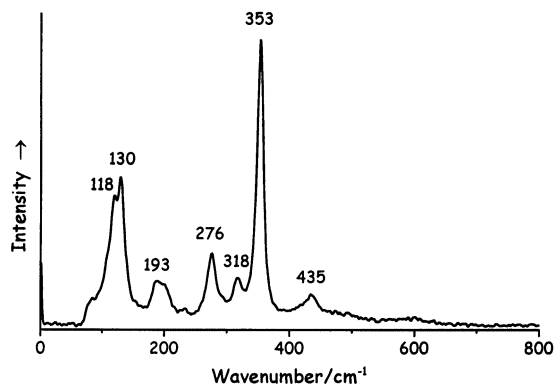
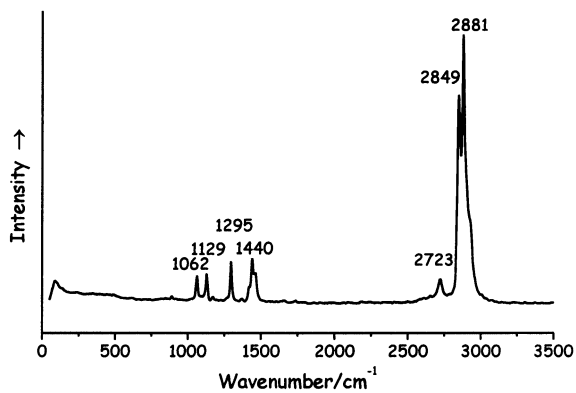
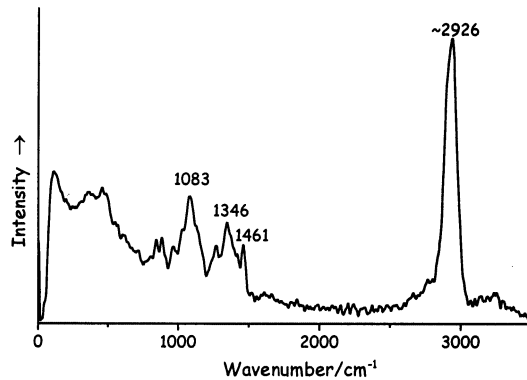
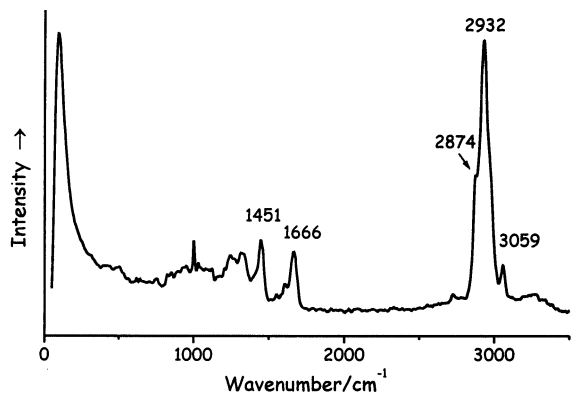
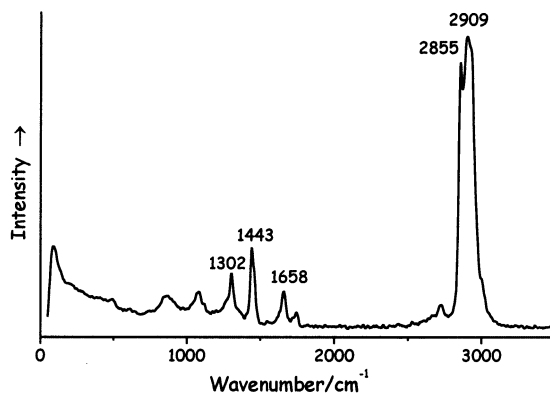
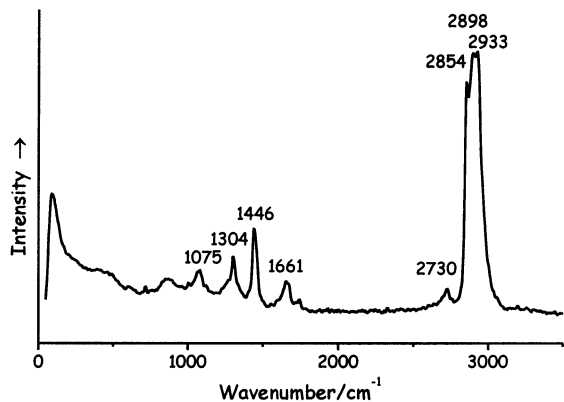
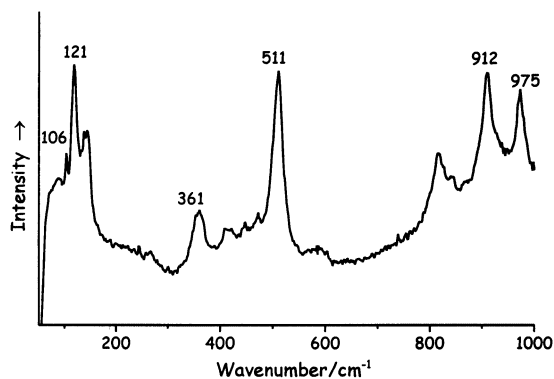
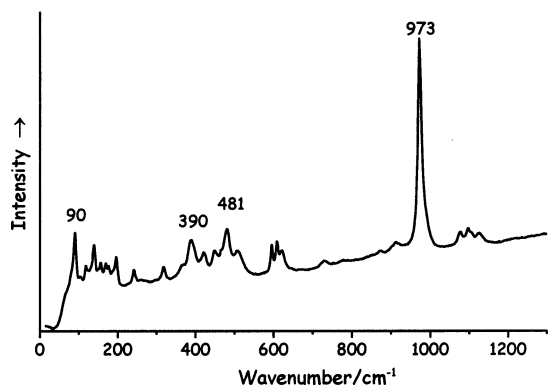
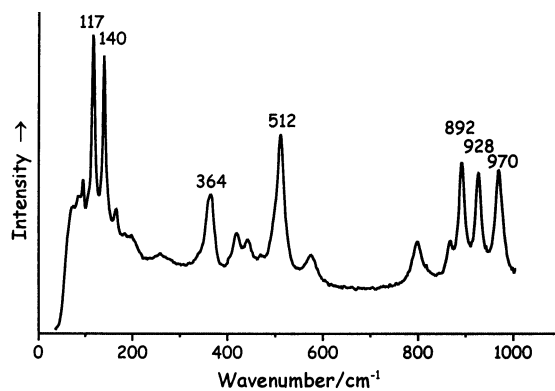
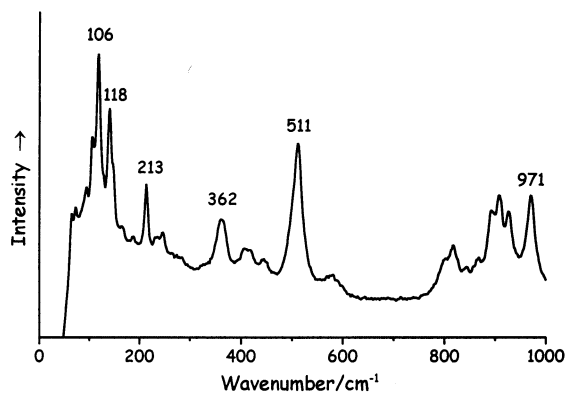
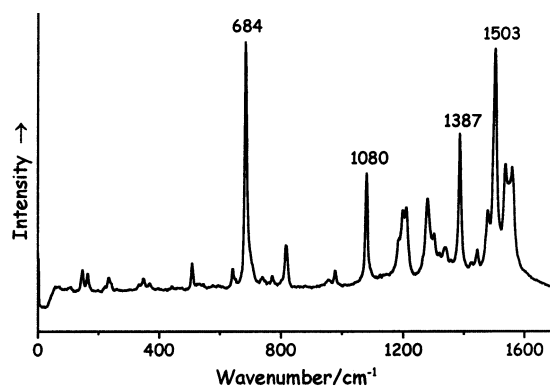
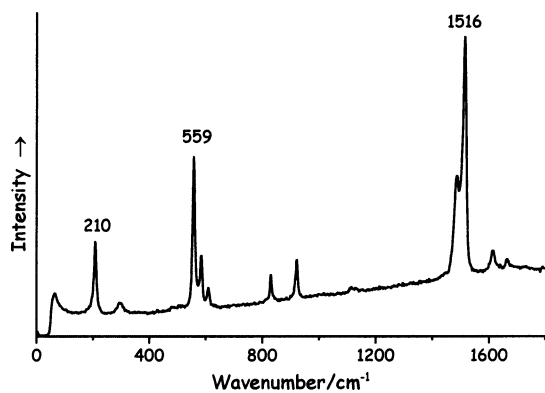
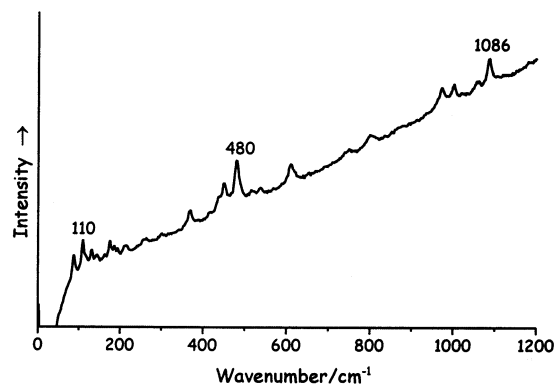
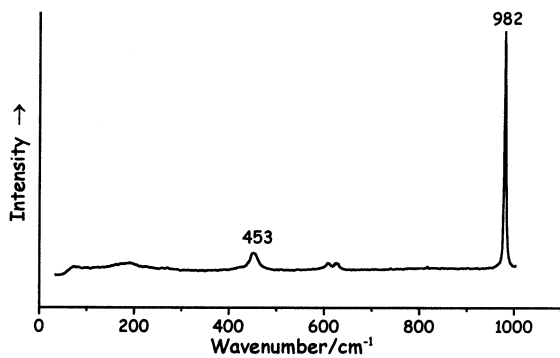
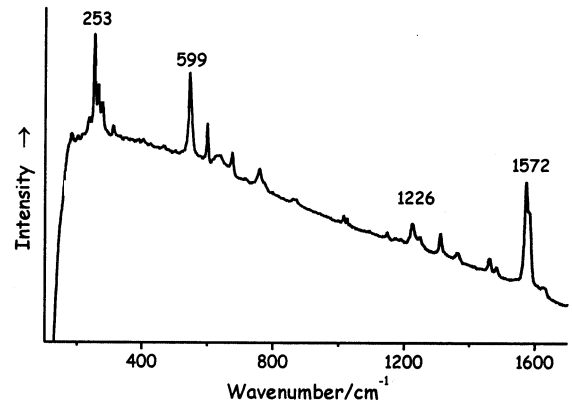
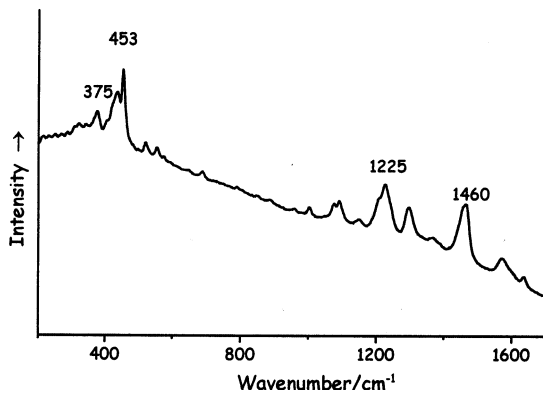
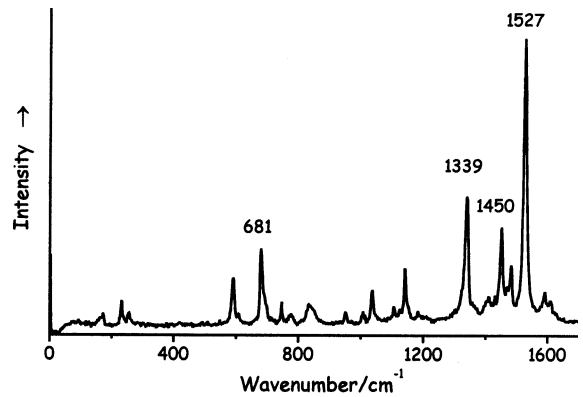
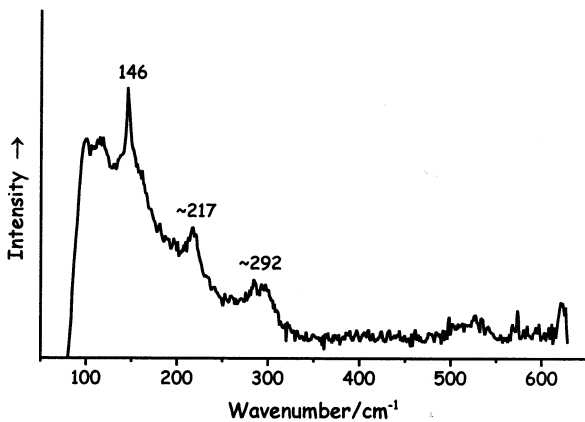
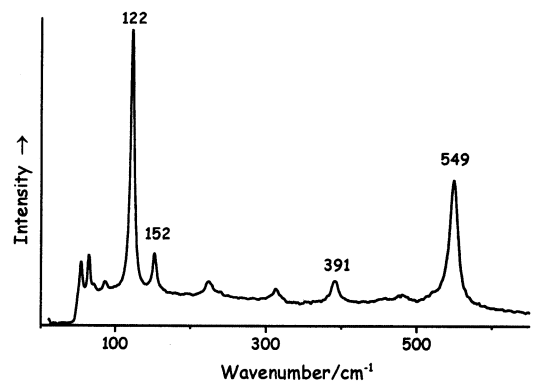
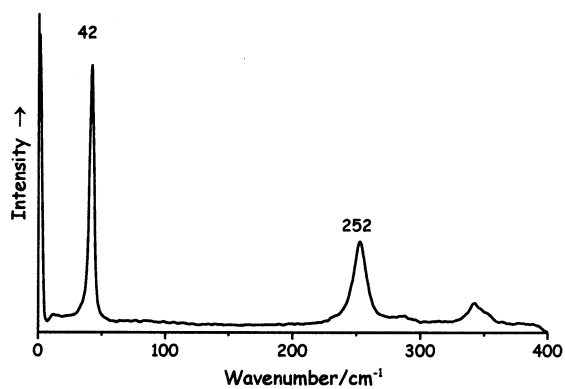
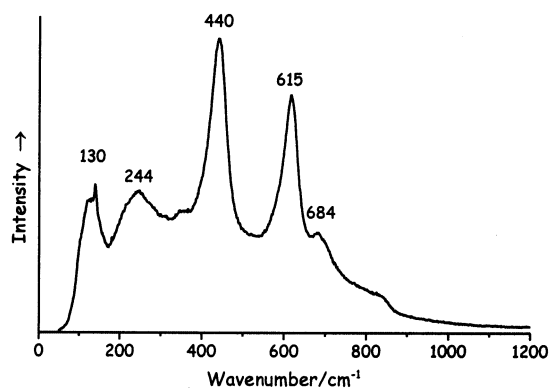
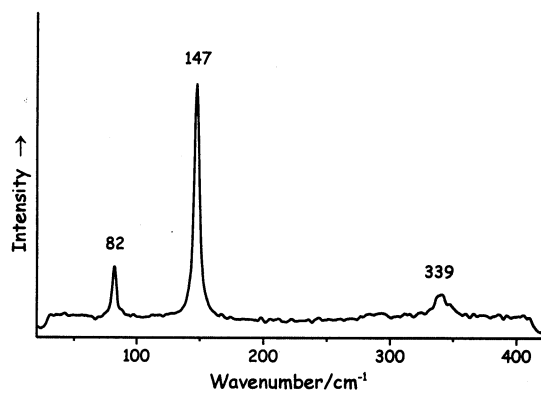
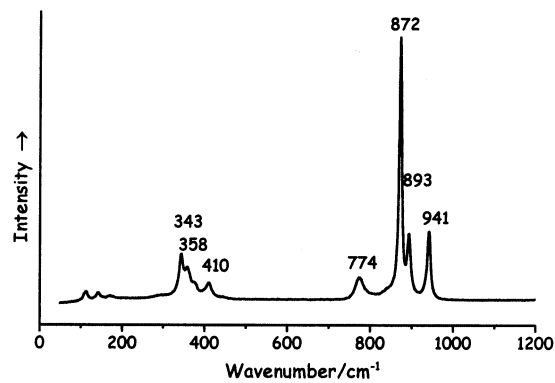
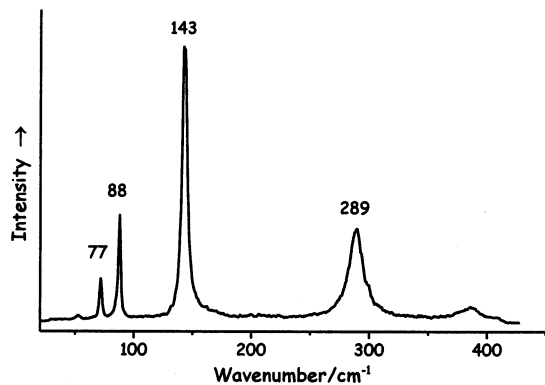
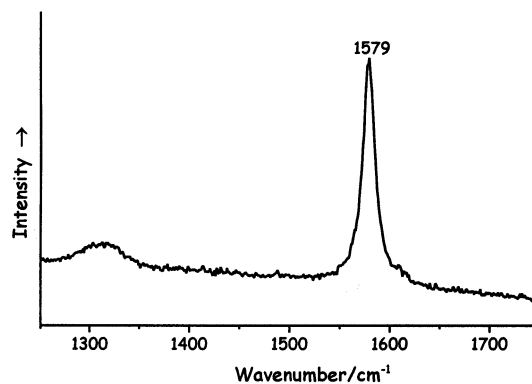


Fig. 55. Tin(II) chloride dihydrate, $\lambda_0 = 1064$ nm, 16 mW.

Fig. 56. Beeswax, $\lambda_0 = 1064$ nm, 130 mW.Fig. 59. Gum arabic, $\lambda_0 = 1064$ nm, 80 mW.Fig. 57. Egg white, $\lambda_0 = 1064$ nm, 130 mW.Fig. 60. Linseed oil, $\lambda_0 = 1064$ nm, 130 mW.Fig. 58. Egg yolk, $\lambda_0 = 1064$ nm, 130 mW.Fig. 61. Atacamite, $\lambda_0 = 514.5$ nm, 0.5 mW.

Fig. 62. Brochantite, $\lambda_0 = 514.5$ nm, 0.5 mW.Fig. 65. Paratacamite, $\lambda_0 = 514.5$ nm, 0.5 mW.Fig. 63. Copper chloride, $\lambda_0 = 514.5$ nm, 0.5 mW.Fig. 66. Phthalocyanine green, $\lambda_0 = 514.5$ nm, 0.5 mW.Fig. 64. Copper oxalate dihydrate, $\lambda_0 = 514.5$ nm, 0.5 mW.Fig. 67. Pseudomalachite, $\lambda_0 = 514.5$ nm, 0.5 mW.

Fig. 68. Tutton salt, $\lambda_0 = 514.5$ nm, 0.5 mW.Fig. 71. Indigo, $\lambda_0 = 780$ nm, 1 mW.Fig. 69. Carminic acid, $\lambda_0 = 780.0$ nm, 5 mW.Fig. 72. Phthalocyanine blue, $\lambda_0 = 514.5$ nm, 1 mW.Fig. 70. Cuprite, $\lambda_0 = 632.8$ nm, 0.2 mW.Fig. 73. Red lead, $\lambda_0 = 647.1$ nm, 1 mW.

Fig. 74. Vermilion, $\lambda_0 = 647.1$ nm, 1 mW.Fig. 77. Nickel titanium yellow, $\lambda_0 = 632.8$ nm, 0.5 mW.Fig. 75. Litharge, $\lambda_0 = 647.1$ nm, 1 mW.Fig. 78. Zinc yellow, $\lambda_0 = 632.8$ nm, 0.5 mW.Fig. 76. Massicot, $\lambda_0 = 647.1$ nm, 1 mW.Fig. 79. Graphite, $\lambda_0 = 780$ nm, 5 mW.

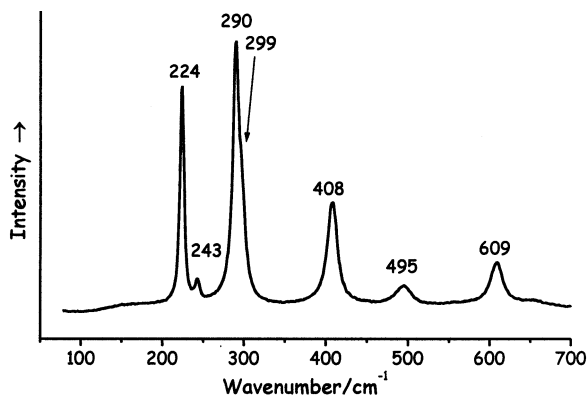


Fig. 80. Haematite, $\lambda_0 = 632.8$ nm, 2 mW.

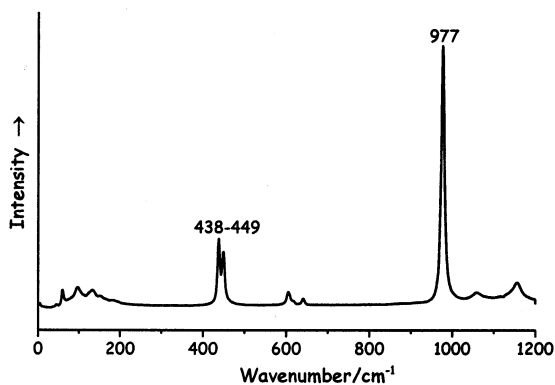


Fig. 81. Lead sulfate, $\lambda_0 = 514.5$ nm, 2 mW.

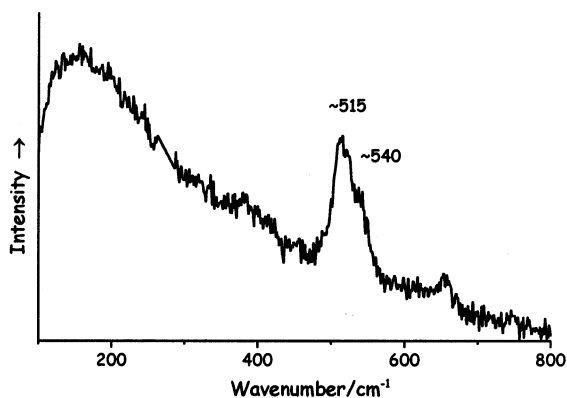


Fig. 82. Plattnerite, $\lambda_0 = 632.8$ nm, 2 mW.

pigments within group one and those collected using visible excitation have also been arranged by colour. The calibrated band wavenumbers

(Raman shift/ cm^{-1}) and relative intensities (uncorrected for spectral response) are listed in Tables 1–12. The tables also indicate the excitation wavelength used, the resolution, the power at the sample, whether the pigment is a mineral or, if synthetic, the date of its earliest manufacture or known use. A list of the available tables follows:

Table 1: FT-Raman spectra of blue pigments.

Table 2: FT-Raman spectra of red pigments.

Table 3: FT-Raman spectra of white pigments.

Table 4: FT-Raman spectra of yellow pigments.

Table 5: FT-Raman spectra of modern synthetic pigments.

Table 6: FT-Raman spectra of minerals and other materials.

Table 7: FT-Raman spectra of binding media and varnishes.

Table 8: List of materials with no detectable FT-Raman signal.

Table 9: Raman spectra of green pigments with visible excitation.

Table 10: Raman spectra of red and blue pigments with visible excitation.

Table 11: Raman spectra of yellow pigments with visible excitation.

Table 12: Raman spectra of miscellaneous materials with visible excitation.

The use of FT-Raman microscopy makes it generally possible to detect substances in trace amounts, for example in the analysis of the white materials used to prepare the paper or the parchment for a manuscript before writing or painting on it. In most cases, the surface of the page had been smoothed with a so-called 'primer', usually calcium sulfate or calcium carbonate, in order to make it more opaque and white, and ready to absorb the inks and the pigments. It is difficult to obtain a Raman spectrum from these materials on the surfaces of pages using visible excitation, because some paper fibres fluoresce intensely under these conditions, and also because the white materials are extremely dilute. By contrast, when FT-Raman microscopy is employed, any white material on the surface of the page gives an excellent spectrum.

This paper shows that this technique can be applied successfully to the analysis and identifica-

tion of most pigments. However, some pigments, e.g. those containing iron and copper, may fluoresce on excitation with near infrared radiation, and therefore may not be identifiable by FT-Raman spectroscopy. Fortunately, other copper-based pigments containing a limited amount of copper, such as Egyptian blue [23,32] and the phthalocyanine pigments [33,34], are able to be identified by this technique.

Other possible applications of Raman microscopy include the analysis of corrosion films on degraded metals [22]. It is very well known for example that, in marine environments, copper objects develop an incrustation composed mainly of basic copper chlorides, such as atacamite and paratacamite [35]. However, environmental pollution is also a major cause of decay of metallic art objects [36–38] such as monuments and statues, one of the most evident signs of which being the formation of a patina of corrosion products on the surface of metallic artefacts. The characterisation of these products is essential in order to identify the best procedures for the restoration and consolidation of the degraded materials. The study of corrosion products can also help in understanding how the environmental conditions and pollution can affect a work of art which is situated in the open air. The Raman analysis of the patina on the surface of corroded artefacts can reveal the cause of the degradation and help in finding the best restoration procedures. Raman microscopic analysis of a sample of corroded bronze has demonstrated that the technique can successfully provide fast and often unambiguous results on bronze corrosion products [22]. Prior to this study, however, it was necessary to collect reference spectra of possible corrosion products of bronze. Some such products are well known, and have been extensively characterised in the past, e.g. the basic copper carbonates malachite and azurite, $\text{CuCO}_3 \cdot \text{Cu}(\text{OH})_2$ and $2\text{CuCO}_3 \cdot \text{Cu}(\text{OH})_2$, respectively, and the basic copper chloride atacamite, $\text{CuCl}_2 \cdot 3\text{Cu}(\text{OH})_2$. The Raman spectra of other such compounds have also been collected here, and are shown in Figs. 61–65, 67 and 68. The Raman bands and the experimental conditions employed for the analyses are shown in Table 8.

The white pigments analysed include anatase and rutile, the most common crystalline modifications of titanium dioxide TiO_2 . They occur in nature as minerals, but always contain some inclusions that cause them to be dark red or black. It was only early in the 20th century that industrial processes were developed for the manufacture of pure white anatase (1923) and rutile (1947). These oxides have proven to be exceptionally good date markers for distinguishing between ancient and modern papyri [34].

This database also includes the spectra of selected modern organic pigments first synthesised in the 20th century, such as phthalocyanine blue and green and compounds belonging to the family of the azo, quinacridone and naphthol pigments. To date more than one thousand modern synthetic pigments have been synthesised, of which the Raman spectra of some were reported [39] as the present database was being assembled.

Tables 6 and 7 contain the spectra of selected materials other than pigments that can be found on works of art. These include common minerals, mainly carbonates and sulfates, and some binding media such as gum arabic. Until recently it was thought that Raman microscopy could only be useful in the identification of pigments on a work of art, and that a binding medium would be in the best case undetectable (for example gum arabic) or in the worst case cause overwhelming fluorescence (for example an oil-based medium). Information about the binding media and varnishes was usually sought by appeal to techniques such as FT-IR or gas chromatography. However, both conventional (780 nm excitation [40]) as well as FT (1064 nm excitation) Raman microscopy have proved to be sensitive probes of binding media, varnishes and pigments (this work) and of gums [41]. The identification of these organic materials is extremely important for restoration and conservation purposes: some solvents commonly employed by restorers in the cleaning of paintings can attack one binding medium but not another, and therefore have to be chosen carefully in order to avoid undesired chemical reactions on the work of art. Moreover, the presence of one binding medium or varnish instead of another may carry important information pertaining to the date and provenance of a work of art.

4. Conclusion

The FT-Raman spectra of 60 pigments and related materials have been collected and arranged into a spectroscopic library. Twenty-two Raman spectra collected using conventional Raman microscopy with visible excitation complete this collection and supplement the earlier database [23]. It has become evident that one major advantage of FT-Raman microscopy over grating spectroscopy is that the whole of the wavenumber range could be covered with each scan. Also, the calibration proved to be extremely consistent over time, resulting in considerable saving of time compared to other instruments in which each spectrum has to be recorded twice, with and without calibration lines. Excellent FT-Raman spectra could be collected from materials such as organic pigments and dyestuffs that either decompose or fluoresce under visible excitation.

One disadvantage of FT-Raman spectroscopy is that the ν^4 factor works greatly against it, necessitating longer scans and higher laser powers than for visible excitation. Moreover, compounds containing either iron or copper which have electronic absorption bands in the near-infrared region, do fluoresce or even burn in the beam when excited at 1064 nm.

Acknowledgements

We are indebted to the EPSRC and the ULIRS for financial support, to the European Commission for the award of a Marie Curie fellowship (to L.B.), to LGC for use of their Renishaw Raman System 1000 spectrometer, and to Dr Paul Turner, J. Gast and Bruker UK Ltd for the loan of a RFS 100/S FT-Raman spectrometer.

References

- [1] L. Burgio, R.J.H. Clark, T. Stratoudaki, M. Doulgeridis, D. Anglos, *Appl. Spectrosc.* 54 (2000) 463.
- [2] B.J. Marquardt, D.S. Stratis, D.A. Cremers, S.M. Angel, *Appl. Spectrosc.* 52 (1998) 1148.
- [3] D. Anglos, M. Solomidou, I. Zergioti, V. Zafiropoulos, T.G. Papazoglou, C. Fotakis, *Appl. Spectrosc.* 50 (1996) 1331.
- [4] T. Tuurnala, A. Hautojärvi, K. Harva, *Stud. Conserv.* 30 (1985) 93.
- [5] L. Busotti, M.P. Carboncini, E. Castellucci, L. Giuntini, P.A. Mandò, *Stud. Conserv.* 42 (1997) 83.
- [6] T. Calligaro, J.-C. Dran, H. Hamon, B. Moignard, J. Salomon, *Nucl. Inst. Methods Phys. Res. B* 136–138 (1998) 339 Related papers pp. 846 and 869.
- [7] B. Guineau, *Stud. Conserv.* 29 (1984) 35.
- [8] B. Guineau, *Stud. Conserv.* 34 (1989) 38.
- [9] D.J. Gardiner, B.W. Singer, J.P. Derow, *Pap. Conserv.* 17 (1993) 13.
- [10] R. Davey, D.J. Gardiner, B.W. Singer, M. Spokes, *J. Raman Spectrosc.* 25 (1994) 53.
- [11] C. Coupry, A. Lautie, M. Revault, J. Dufilho, *J. Raman Spectrosc.* 25 (1994) 89.
- [12] R.J.H. Clark, *Chem. Soc. Rev.* 24 (1995) 187.
- [13] S.P. Best, R.J.H. Clark, M.A.M. Daniels, C.A. Porter, R. Withnall, *Stud. Conserv.* 40 (1995) 31.
- [14] C. Coupry, G. Sagon, P. Gorguet-Ballesteros, *J. Raman Spectrosc.* 28 (1997) 85.
- [15] R.J.H. Clark, P.J. Gibbs, K.R. Seddon, N.M. Brovenko, Y.A. Petrosyan, *J. Raman Spectrosc.* 28 (1997) 91.
- [16] L. Burgio, D.A. Ciomartan, R.J.H. Clark, *J. Raman Spectrosc.* 28 (1997) 79.
- [17] L. Burgio, D.A. Ciomartan, R.J.H. Clark, *J. Mol. Struct.* 405 (1997) 1.
- [18] R.J.H. Clark, P.J. Gibbs, *Chem. Commun.* (1997) 1003.
- [19] R.J.H. Clark, P.J. Gibbs, *Anal. Chem.* 70 (1998) 99A.
- [20] H.G.M. Edwards, L. Drummond, J. Russ, *J. Raman Spectrosc.* 30 (1999) 421.
- [21] F.R. Perez, H.G.M. Edwards, A. Rivas, L. Drummond, *J. Raman Spectrosc.* 30 (1999) 301.
- [22] L. Burgio, PhD Thesis, University of London (2000).
- [23] I.M. Bell, R.J.H. Clark, P.J. Gibbs, *Spectrochim. Acta* 53A (1997) 2159.
- [24] Cennino d'Andrea Cennini, *The Craftsman's Handbook. Il Libro dell'Arte*, translated by D.V. Thompson, Dover, New York, 1954.
- [25] D.V. Thompson, *The Materials and Techniques of Medieval Painting*, Dover, New York, 1956.
- [26] R.J. Gettens, G.L. Stout, *Painting Materials*, Dover publications, New York, 1966.
- [27] K. Wehlte, *The Materials and Techniques of Painting*, Van Nostrand Reinhold Co. Ltd, New York, 1975.
- [28] R.L. Feller (Ed.), *Artists' Pigments, a Handbook of their History and Characteristics*, vol. 1, Cambridge University Press, Cambridge, 1986.
- [29] A. Roy (Ed.), *Artists' Pigments, a Handbook of their History and Characteristics*, vol. 2, Oxford University Press, Oxford, 1994.
- [30] E. West Fitzhugh (Ed.), *Artists' Pigments, a Handbook of their History and Characteristics*, vol. 3, Oxford University Press, Oxford, 1997.
- [31] The spectra contained in this paper constitute Appendix A of the PhD thesis of L.B.
- [32] C. Coupry, S. Pages Camagna, S. Colinart, *J. Raman Spectrosc.* 30 (1999) 313.

- [33] L.I. McCann, K. Trentelman, T. Possley, B. Golding, J. Raman Spectrosc. 30 (1999) 121.
- [34] L. Burgio, R.J.H. Clark, J. Raman Spectrosc. 31 (2000) 395.
- [35] L. Veleva, P. Quintana, R. Ramanauskas, R. Pomes, L. Maldonado, Electrochim. Acta 41 (1996) 1641.
- [36] H. Strandberg, L.G. Johansson, J. Electrochem. Soc. 144 (1997) 2334.
- [37] A. Salnick, W. Faubel, Prog. Nat. Sci. 6 (1996) S14.
- [38] J.Y. Malvault, J. Lopitaux, D. Delhay, M. Lenglet, J. Appl. Electrochem. 25 (1995) 841.
- [39] P. Vandenaabeele, L. Moens, H.G.M. Edwards, J. Raman Spectrosc. 31 (2000) 509.
- [40] P. Vandenaabeele, B. Wehling, L. Moens, H. Edwards, M. De Reu, G. Van Hooydonk, Anal. Chim. Acta 407 (2000) 261.
- [41] H.G.M. Edwards, M.J. Falk, M.G. Sibley, J. Alvarez-Benedi, F. Rull, Spectrochim. Acta Part A 54 (1998) 903.